The Meteoritical Society

Meteoritics & Planetary Science 43, Nr 11, 1841–1859 (2008)
Abstract available online at http://meteoritics.org

Helium loss from Martian meteorites mainly induced by shock metamorphism: Evidence from new data and a literature compilation

S. P. SCHWENZER[1, 6*], J. FRITZ[2, 3], D. STÖFFLER[2], M. TRIELOFF[3], M. AMINI[1, 4], A. GRESHAKE[2], S. HERRMANN[1], K. HERWIG[1], K. P. JOCHUM[1], R. K. MOHAPATRA[1, 5], B. STOLL[1], and U. OTT[1]

[1]Max-Planck-Institut für Chemie, J.-J. Becher-Weg 27, D-55128 Mainz, Germany
[2]Museum für Naturkunde, Leibniz Institut für Evolutions- und Biodiversitätsforschung an der Humboldt-Universität zu Berlin, Invalidenstrasse 43, D-10115 Berlin, Germany
[3]Universität Heidelberg, Institut für Geowissenschaften, Im Neuenheimer Feld 236, D-69120 Heidelberg, Germany
[4]Present address: Saskatchewan Isotope Laboratory, Department of Geological Sciences, University of Saskatchewan, 114 Science Place, Saskatoon, SK S7N 5E2, Canada
[5]Present Address: Department of Earth Sciences, University of Ottawa (Marion Hall), 140 Louis Pasteur, Ottawa, Ontario, Canada
[6]Present address: Lunar and Planetary Institute, 3600 Bay Area Blvd., Houston, Texas 77058, USA
*Corresponding author. E-mail: schwenzer@lpi.usra.edu
Online appendix is available at http://meteoritics.org/Online%20Supplements.htm

(Received 29 February 2008; revision accepted 25 June 2008)

Abstract–Noble gas data from Martian meteorites have provided key constraints about their origin and evolution, and their parent body. These meteorites have witnessed varying shock metamorphic overprinting (at least 5 to 14 GPa for the nakhlites and up to 45–55 GPa (e.g., the lherzolitic shergottite Allan Hills [ALH] A77005), solar heating, cosmic-ray exposure, and weathering both on Mars and Earth. Influences on the helium budgets of Martian meteorites were evaluated by using a new data set and literature data. Concentrations of ^{3}He, ^{4}He, U, and Th are measured and shock pressures for same sample aliquots of 13 Martian meteorites were determined to asses a possible relationship between shock pressure and helium concentration. Partitioning of ^{4}He into cosmogenic and radiogenic components was performed using the lowest ^{4}He/^{3}He ratio we measured on mineral separates (^{4}He/^{3}He = 4.1, pyroxene of ALHA77005). Our study revealed significant losses of radiogenic ^{4}He. Systematics of cosmogenic ^{3}He and neon led to the conclusion that solar radiation heating during transfer from Mars to Earth and terrestrial weathering can be ruled out as major causes of the observed losses of radiogenic helium in bulk meteorites. For bulk rock we observed a correlation of shock pressure and radiogenic ^{4}He loss, ranging between ~20% for Chassigny and other moderately shocked Martian meteorites up to total loss for meteorites shocked above 40 GPa. A steep increase of loss occurs around 30 GPa, the pressure at which plagioclase transforms to maskelynite. This correlation suggests significant ^{4}He loss induced by shock metamorphism. Noble gas loss in rocks is seen as diffusion due to (1) the temperature increase during shock loading (shock temperature) and (2) the remaining waste heat after adiabatic unloading (post shock temperature). Modeling of ^{4}He diffusion in the main U,Th carrier phase apatite showed that post-shock temperatures of ~300 °C are necessary to explain observed losses. This temperature corresponds to the post-shock temperature calculated for bulk rocks shocked at about 40 GPa. From our investigation, data survey, and modeling, we conclude that the shock event during launch of the meteorites is the principal cause for ^{4}He loss.

INTRODUCTION

Helium Isotopes in Meteorites

Helium in Martian meteorites is important for several reasons: (1) Understanding the radiogenic helium budget would provide us with a powerful dating tool for effects below the closure temperature of the argon system. (2) Cosmogenic helium provides insight into the space travel history of the rock in hand. (3) Helium is the only noble gas that cannot be implanted into the rock in significant amounts as its concentration is low in the Martian atmosphere (see section Helium Incorporation on Mars). It therefore monitors loss mechanism for noble gases without confusion from implantation. Furthermore, helium

and argon budgets of Martian meteorites have been used to shed light on the thermal history of Mars (Shuster and Weiss 2005) arguing that "ambient near-surface temperatures on Mars" unlikely were much higher than the present cold (<0 °C)" for most of the planet's history.

Among the noble gases, helium has the highest diffusion rates through many minerals and glasses (Ozima and Podosek 2002), and therefore its initial inventory is most easily disturbed. In meteorites, the two isotopes (^{3}He, ^{4}He) are of different origin: while ^{3}He is almost completely produced by spallogenic reactions due to cosmic ray irradiation (also termed "cosmogenic"), the cosmogenic contribution to ^{4}He is in almost all cases rather small compared to the radiogenic contribution from U and Th-decay chains. This study addresses the effects on the helium inventory of Martian meteorites, e.g., solar heating, shock metamorphism, and terrestrial weathering. Although the main focus is on the influence of shock metamorphism on the ^{4}He budget, other possible effects on ^{3}He are to be discussed. As almost all ^{3}He is produced during travel in space, it can be used as an indicator for processes acting on the helium budget of a meteorite after launch from Mars. The effects on the two isotopes of helium may vary in their extent due to their different atomic mass (see Trieloff et al. [2005] for such effects on argon isotopes) and also different host minerals, but should be comparable.

Helium loss as a phenomenon in stony meteorites—more specifically in H and L chondrites—has been studied in detail as early as 1966 by Hintenberger et al. (1966, 1967). They observed severe loss of ^{3}He and ^{4}He, especially in metal and pyroxene, while olivine was found to be retentive in most cases. About 50% of spallogenic ^{3}He forms via the precursor isotope tritium (e.g., Leya et al. 2004), which diffuses much faster than helium, especially in metal. Moreover, both ^{3}He and ^{4}He can be lost due to solar heating on near-Sun orbits. Among later studies, Loeken et al. (1992) found two individuals among 18 chondrites with exceptionally low ^{3}He/^{21}Ne ratios, which they conclude to have been caused by ^{3}He (or tritium) loss in near-Sun orbits. Diffusive losses of helium in some H chondrites have also been reported by Schultz and Weber (1996), who suggested two possible reasons: loss due to thermal overprinting on the parent body, and near-Sun heating to temperatures between 100 and 200 °C. They cite as additional support for the latter that all of those which show ^{3}He loss are morning falls. Remarkably, all Martian meteorite falls, for which the time of fall has been documented (Nakhla, Shergotty, and Chassigny; Meyer 2006), are morning falls, which implies the question, if this is testimonial evidence of near solar orbits. Nevertheless, as will be discussed below, solar heating is unlikely to have caused major He loss from Martian meteorites.

In this paper, we discuss the whole set of possible influences that could change the helium budget of Martian meteorites from what was originally caused by U and Th decay to what is observed in the rocks in hand. Our discussion follows the pathway of the meteorite from its emplacement and residence in the Martian near-surface, ejection by impact cratering, space travel, and final terrestrial residence associated with weathering. The mechanisms discussed include incorporation of extraneous helium, pre-irradiation on Mars, shock metamorphism, cosmic ray production, solar heating, and terrestrial weathering. As for petrologic terminology we are using "Martian meteorites" and "SNC meteorites" interchangeably (SNC comes from the names of the three type specimens Shergotty, Nakhla, and Chassigny). We furthermore refer to the groups defined by the SNC type specimens and use the sub-group classification of Goodrich (2002). A more detailed petrology is beyond the necessity for the course of this paper.

Shock Metamorphism

Shock metamorphism was repeatedly suggested to be an important mechanism for helium loss from meteorites (see section Shock Pressure and Noble Gas Loss) and will be an important part of our discussion. Because the effects of shock metamorphism have been sometimes misinterpreted in the literature, we present some introductory basic facts that are critical for the understanding of our study.

Determination of "Equilibration" Shock Pressures

An overview of shock metamorphism in different meteorites and a general classification of the effects including Martian meteorites is given by Stöffler et al. (1988), Bischoff and Stöffler (1992), and most recently by Sharp and De Carli (2006). For more specific discussions of the shock history of Martian meteorites we refer the reader to the references contained in these papers. For pressure and temperature determinations of Martian meteorites we used mainly the data of Fritz et al. (2005a, 2005b) that contains a comprehensive list of shock pressures and calculated shock and post-shock temperatures for 18 of the 32 Martian meteorites known in 2004. A compilation of shock pressure estimates for Martian meteorites is given in Table A1 in the online appendix available at http://meteoritics.org/Online%20Supplements.htm.

To determine the final peak shock pressure ("equilibration shock pressure") experienced by a Martian meteorite, one has to distinguish between (1) shock effects for which the responsible shock pressure has been calibrated by shock recovery experiments with relevant minerals (plagioclase, olivine, and pyroxene), with meteorites (the H chondrite Kernouvé) and/or analog rocks (basalt, gabbro, pyroxenite, dunite; see Reimold and Stöffler 1978; Ostertag 1983; Schmitt 2000, and more references in Stöffler et al. 1991), and (2) shock effects for which exact calibrations are not available. Second, it is necessary to distinguish between shock effects resulting from the final "equilibration" shock pressure achieved in the meteorite as a whole and shock effects resulting from pressure and temperature excursions induced locally by distinct differences in the shock

impedance of the constituent phases, e.g., minerals and/or pores and fissures (Stöffler et al. 1991). The former are the shock effects observed in the main constituent minerals such as plagioclase, olivine, and pyroxene. The latter, classified as "disequilibrium" effects (Stöffler et al. 1991), are melt veins (shock veins) and melt pockets observed typically in mafic and ultramafic rocks. It should be emphasized that the high pressure polymorphs, which occur in or near to melt veins and melt pockets (e.g., Chen et al. 1996; El Goresy et al. 2000, 2003; Beck et al. 2002; Xie and Sharp 2004; Xie et al. 2006a, 2006b), cannot be used as barometers of the "equilibration" shock pressure as they form in very localized, kinetically favored regions characterized by pressure-temperature spikes.

On the basis of the above mentioned calibration data two results were obtained: First, the "equilibration" shock pressures recorded in all analyzed Martian meteorites range from about 5 to 55 GPa (e.g., Fritz et al. 2005a), and, second, melting of mafic to ultramafic rocks resulting in veins and pockets requires local peak shock pressures of at least 70–80 GPa (Stöffler et al. 1986, 1991; Schmitt 2000). In summary, the "equilibration" shock pressure of a meteorite to which we refer in this paper is derived from the shock effects which are ubiquitous throughout the whole meteorite and are observed in the constituent minerals (plagioclase, olivine, pyroxene) which represent the main mass of the meteorite.

Shock Pressure and Noble Gas Loss

Heating of meteorites due to collisions in space as a reason for loss of noble gases was first discussed by Kirsten et al. (1963). After the discovery of shock-implanted gases in the Martian meteorite Elephant Moraine (EET) A79001, recovery of gases in experimentally shocked materials has been studied by two groups (Bogard et al. 1986, 1989; Wiens and Pepin 1988). These studies, of course, focused on gain rather than loss, but also observed that nitrogen and CO_2, helium and in some cases neon were lost. They attribute the loss to diffusion driven by post-shock temperature.

Regarding naturally shocked samples, no systematic study of radiogenic helium contents has been carried out on any terrestrial impact crater structure. The situation is different for meteorites, for which several studies relate noble gas loss to shock metamorphic overprinting: first, evidence for helium loss in hypersthene (= L) chondrites was found in a literature survey, and later extended beyond that (Heymann 1967; Taylor and Heymann 1969). Dodd and Jarosewich (1979) presented a shock classification based on presence of melt inclusions and petrographic characteristics of olivine, and found their inferred shock pressure intensity to correlate with the amounts of ^{4}He and ^{40}Ar. A comprehensive study on Ar-degassing patterns of heavily shocked chondrites is reported by Bogard and Hirsch (1980). The work on chondrites is summarized by Bischoff and Stöffler (1992). They found petrologic evidence that shock metamorphism correlates with the occurrence of interstitial melt as well as with low gas retention ages. The relative abundances of interstitial melt was shown by the same authors (see their Fig. 23; and also Bischoff et al. 1983) to anti-correlate with the concentrations of solar wind implanted ^{4}He and ^{20}Ne. Furthermore, Schultz and Stöffler (1993) compared shock stages in different chondrites with helium data available at that time and found complete loss of—loosely bound—implanted solar wind ^{4}He for ordinary chondrites shocked to more than shock stage S3 (i.e., >10–15 GPa) and severe loss of radiogenic ^{4}He (residing in the volume of mineral grains) in H- and L-chondrites shocked to stages S4 and above (i.e., >25–30 GPa). Obviously, loss of ^{4}He due to shock-metamorphic overprint is the rule rather than the exception in meteorites showing petrographic evidence for shock.

An example for a more complicated interplay of different types of helium loss was given by Eugster et al. (1993): Some chondrites lost ^{3}He and ^{4}He, which the authors attribute to either near solar orbits or a late collisional breakup event, others lost ^{4}He only, which must be associated with processes on their parent body. In addition, Schultz and Weber (1996) concluded from their measurement of light noble gases in a series of H chondrites solar heating on near solar orbits is the reason for the observed deficit.

As for Martian meteorites, loss of noble gases has been reported for Lewis Cliff (LEW) 88516 (^{4}He, Ott and Löhr 1992) and Queen Alexandra Range (QUE) 94201 (^{4}He and ^{40}Ar, Swindle et al. 1996). Both meteorites have been shocked to 45 GPa (cf. Table A1, Fritz et al. 2005). Walton et al. (2007) found the concentration of Martian atmosphere being highest in shock melt pockets, lower in shock veins and "not" present in magmatic minerals of Zagami and Northwest Africa (NWA) 1068. Dar al Gani (DaG) 476 shows the same trend in principle, but the picture is less clear, most probably due to weathering effects. These findings shed light on the fact that change of the noble gas inventories is among the consequences of shock metamorphism.

Furthermore, from observations of the Los Angeles, Sayh al Uhaymir (SaU) 150, and DaG 476 Martian meteorites and dynamic crystallization experiments performed on synthetic glass analogues of shock melt, Walton et al. (2006) deduce that "~20–30% of the trapped Martian atmospheric argon may be lost" from the melt pockets due to diffusive transport during subsequent crystallization. Their findings shed light also on the complementary process: implantation of Martian atmosphere. Implantation thwarts any attempt to estimate ^{40}Ar loss from shergottites, especially as the indigenous and the implanted signatures are indistinguishable in their release patterns (Bogard et al. 1989). Therefore, argon will not be further discussed in this paper. For helium, the existence of a correlation between loss of ^{4}He and shock pressure has been suggested earlier (Schwenzer 2004; Schwenzer et al. 2004) and ^{4}He has been found to be deficient compared to the expected amount in the shergottites Shergotty, Zagami, and EETA79001 (Lithology A) (Schwenzer et al. 2007). An interesting aspect is added by the study of Min et al. (2004),

who find U/Th-He ages of merrillites and chlorapatites from Los Angeles to be indistinguishable from the cosmic-ray exposure age. They conclude that shock metamorphism completely reset the U/Th-He system and the launching event was close in time to the metamorphic overprint.

To summarize, previous studies already indicate loss of radiogenic helium due to shock metamorphism, but several problems remain: first, most U,Th,-He data were obtained on different portions of the respective meteorites, not on aliquots, thereby potentially adulterating ^{4}He loss and the potential correlation with shock pressure. Second, for many meteorites the timing of the shock event and their pre-shock U,Th-He age is not clear. It furthermore is unclear if they were affected by late post-shock thermal metamorphism, e.g., when covered by impact melts on their parent body. These problems arise because meteorites from small asteroids can be launched by late low energetic events not recorded by clear signs of impact metamorphism. This is different for Martian meteorites: they can only be launched by highly energetic shock events (that likely dominate previous events). The launching event occurred at a rather late point-of-time in the Martian meteorites' history, which is well-defined by the cosmic ray exposure age. After launch further thermal metamorphism is virtually impossible (except for very mild solar heating). These circumstances make it favorable to focus a study on aliquotted samples of Martian meteorites with well-known ejection and crystallization ages.

EXPERIMENTAL METHODS AND DATA SETS

This work combines new He, U, Th data on 13 SNC-meteorites with literature data on 20 SNC meteorites as follows:

Helium

Helium measurements in 13 bulk meteorite samples from all petrologic classes of the Martian meteorites (details are in Table A2 in the online appendix) were performed in the noble gas laboratory at the Max-Planck-Institut für Chemie, Mainz. Approximately 50 mg of powdered sample were wrapped in Ni foil, and analyzed with procedures outlined in Verchovsky et al. (1993) and Schwenzer (2004). Gas extraction was by stepwise pyrolysis. Typical blanks were $4.5^{*}10^{-9}$ ccSTP of ^{4}He and $4.3^{*}10^{-13}$ ccSTP of ^{3}He. Twelve of the 13 samples were measured in the framework of a comprehensive study on SNC-meteorites (Schwenzer 2004). LEW 88516 was measured earlier (Ott and Löhr 1992).

Besides our own data, we examine data for bulk Martian meteorites from the compilation of Schultz and Franke (2004). We also used the results for the new chassignite NWA 2737 by Marty et al. (2006). In cases where the compilation (Schultz and Franke 2004) lists more than one analysis, an average content was used for both ^{4}He and ^{3}He. Ne data are needed to assess losses of cosmogenic He from the cosmogenic He/Ne ratio and were taken from the same sources. Data from Bogard et al. (1984) (and with them the only data on EETA 79001 lithology B) were excluded, because these authors do not provide errors and the nominal Ne isotopic ratios are in a range that appears physically impossible in some cases (Leya et al. 2000).

Expected cosmogenic ^{3}He was calculated using galactic cosmic ray (GCR) production rates based on the data set of Leya et al. (2000) and data in Table 1. In contrast to other calculations of cosmogenic production rates (Eugster 1988; Eugster et al. 1997), in the data set by Leya and co-workers the complete chemical composition of major elements is taken into account.

To calculate cosmogenic ^{3}He from cosmic ray interaction, we computed individual chemical compositions of each of the 22 meteorites by averaging abundances from the compilation of Lodders (1998). Exceptions are as follows:

1. Lafayette: the only value for Na has been obtained on fusion crust by Boctor et al. (1976). Because fusion crust may be depleted in Na, a bulk rock value of 0.42% (by weight) has been adopted, based on modal mineral abundances and the average Na_2O contents of plagioclase and augite (Treiman 2005, Allan H. Treiman personal communication).
2. SaU 005 and DaG 476: Data from Dreibus et al. (2000) and from Zipfel et al. (2000) are used.
3. Yamato (Y-) 000593 and NWA 817: Data listed by Treiman (2005) are used.
4. NWA 2737: Data from Beck et al. (2006) are used.
5. Los Angeles: Data from Rubin et al. (2000) are used.

To derive the ^{3}He produced in the meteorites, the exposure ages and estimates for the radii are also needed (see Table 1). The exact sizes of the meteoroids are unknown, of course. For most of the specimens under consideration, estimates from radiogenic nuclides and/or noble gas measurements exist. The results of these studies are included in Table 1. A lower limit for the meteorite radius is defined by the size of the specimen in hand. Therefore, the radius range used for our calculations was taken as the minimum (cf. Table 1) up to 40 cm. A maximum value of 40 cm was chosen, because, with production rates declining again for larger radii, including them does not lead to an enlargement of total range (except for very large specimens which, however, can be ruled out from neon isotope systematics). The results (Fig. 1) cover the range of expected ^{3}He amounts including the different shielding depths and radii.

Partitioning of Measured ^{4}He into Its Cosmogenic and Radiogenic Components

^{4}He stems from cosmogenic as well as radiogenic sources. To arrive at the observed radiogenic amount of ^{4}He one has to take into account the cosmogenic production of ^{4}He, which is subtracted from the observed ^{4}He amount.

Table 1. Data base for calculating the ranges of ^{3}He production with meteorites chemistry and production rates from Leya et al. (2001) in Fig. 1. Eugster et al. (2002) from their ^{81}Kr-studies give minimum radii of 20–25 cm for the following Martian meteorites: QUE 94201, SaU 005, Shergotty, Zagami, Nakhla, Chassigny.

Name	Class[a]	Recovered mass[b] (kg)	Density[c] (g/cm³)	Min. radius[d] (cm)	Min. category[e] (cm)	Radii from literature (cm)	Exposure age[f]
ALH 77005	Lherzolitic shergottite	0.482	3	3.4	5	~4[bha] 10[schn] 5[bas] ~13[bee1] 20–30 [fri]	3.2* (3.8)
ALHA 84001	Orthopyroxenite	1.93	3.3	5.2	5	25[schn] 15[bas]	13.7* (14.7)
Chassigny	Chassignite	4	4.7	5.9	5	>24[eug] 25–40[bas] 15–20[bee2]	11.6* (11.1)
Dar al Gani 476	Olivine phyric shergottite	>6, 7 pieces	3	7.8	10	>10–12[nis1]	1.26 (1.24)
Dhofar 019	Olivine phyric shergottite	1.056	3	4.2	5	>7[nis2]	18.1 (19.8)
EETA 79001, Lith. A	Olivine phyric shergottite	7.94	3	8.6	10	~10[bha] 10–15[schn] 25–65[bas]	0.55* (0.73)
Governador Valadares	Nakhlite	0.158	3.3	2.3	5	40[bas]	10.1* (10.0)
Lafayette	Nakhlite	0.8	3.3	3.9	5		11.4* (11.9)
LEW 88516	Lherzolitic shergottite	0.0132	3	1.0	5	25[schn] >22–25[eug]	3.5 (3.9)
Los Angeles	Basaltic shergottite	0.698	3	3.8	5	20–40[nis3]	3.0 (3.0)
Nakhla	Nakhlite	10	3.3	9.0	10	>22[eug] 40[bas]	11.6* (10.8)
NWA 817	Nakhlite	0.104	3.3	2.0	5		9.7
NWA 2737	Chassignite	0.611	4	3.3	5		10.5
QUE 94201	Basaltic shergottite	0.012	3	1.0	5	25[schn] >24[eug]	2.6* (2.8)
Sayh al Uhaymir 005	Olivine phyric shergottite	>10, about 7 pieces	3	9.3	10	>25[eug] 15–50[bas] 10–12[pae]	1.5 (1.2)
Shergotty	Basaltic shergottite	5	3	7.4	10	~12[bha] >23[eug] 40[bas]	2.7* (3.0)
Zagami	Basaltic shergottite	~18	3	~11.3	15	25[schn] >23[eug]	2.7* (3.0)

[a]Goodrich (2002). [b]Meyer (2006). [c]Estimated from mineralogical composition. [d]Radius of a sphere with the mass in col. 3 and density in col. 4. [e]The data in Leya et al. (2000) for radii: 5, 10, 15, 25, 32, 40, 50, 65, and 85 cm. For "minimum category" we have used the radius, closest to the minimum radius in col. 5. [f]Exposure ages are from compilations Eugster et al. (1997), these are marked with an asterisk. Eugster et al. (2002) report ejection ages (i.e., exposure age plus terrestrial age), which are given in brackets for comparison. The terrestrial age is important, if the ejection age is very short, i.e., for EETA79001, mostly. Exceptions are as follows: DaG 476 Zipfel et al. (2000); Dhofar 019 Shukolyukov et al. (2000); LEW 88516 Ott and Löhr (1992); Los Angeles Eugster et al. (2000); NWA 817 Marty et al. (2001); NWA 2737 Marty et al. (2006); SaU 005 Pätsch et al. (2000). Comparing the given mean values to 81-Kr ages from Eugster et al. (2002) the values for ALH 84001,Chassigny, Los Angeles, Nakhla, QUE 94201, Shergotty, and Zagami agree within measurement errors of T81, whereby T81 is higher for the following individuals: ALH 84001, Los Angeles, Shergotty, and Zagami, for the other T81 is lower than the mean given above.

[bas] Bastian (2004), [bha] Bhandari et al. (1986), [eug] Eugster et al. (2002), [nis1] Nishiizumi et al. (2001), [nis2] Nishiizumi et al. (2002), [nis3] Nishiizumi et al. (2000), [pae] Pätsch et al. (2000), [schn] Schnabel et al. (2001); [bee1] Beech et al. 2008; [bee2] Beech et al. 2007; [fri] Fritz et al. 2005a

Details of the possibility of pre-irradiation and cosmogenic ^{4}He will be discussed in chapters 3.2 and 3.4, respectively. The ratio of $(^4He/^3He)_{cosm}$ reported by Heymann (1967) is 5.2 ± 0.3, while Alexeev (1998) report 6.1 ± 0.3 and Welten et al. (2003) 6.2 ± 0.2. Alexeev (2005) reports a variation in L-chondrites of 5.5 ± 0.8 (Antarctic finds) to 6.7 ± 0.5 (falls). In our case the lowest measured ratio is 4.1 (pyroxene of ALHA77005; Schwenzer et al. 2006), which we take as pure cosmogenic composition for partitioning ^{4}He into cosmogenic and radiogenic components. Choosing one of the other values would change the resulting numbers of concentrations and loss of radiogenic He; however, our basic conclusions are not affected by such a different choice.

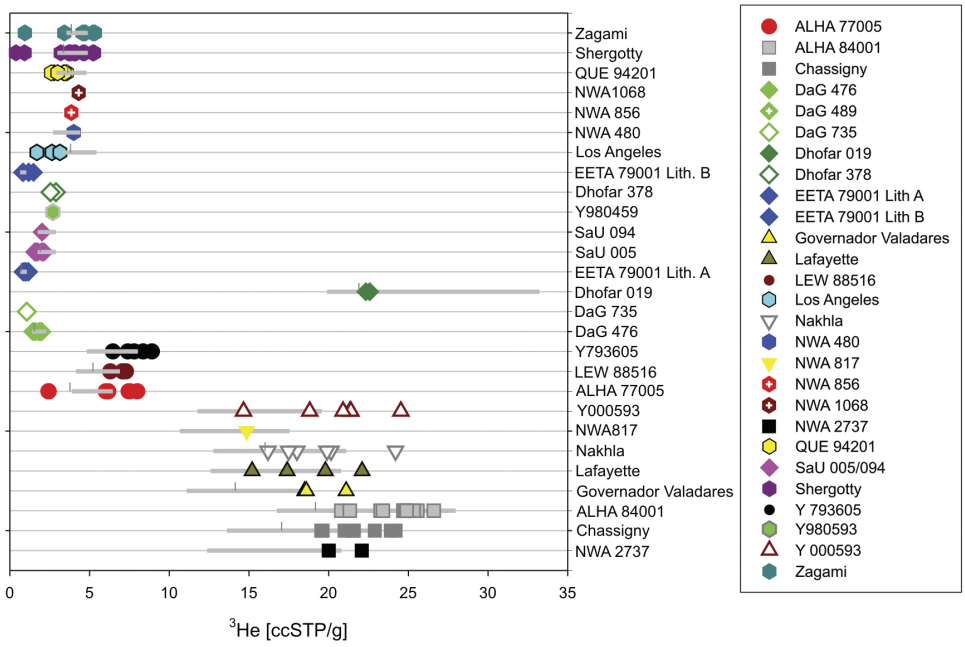

Fig. 1. ^{3}He contents (Literature data, Schultz and Franke 2004) of Martian meteorites grouped by classes (after Goodrich 2002). The thick grey line shows the range of possible ^{3}He content (calculated with the model of Leya et al. 2000) according to meteorite size, shielding depth and exposure age (see also Table 3). The size range is the minimum range from the find mass (see Table 1) up to 40 cm, as the production has a maximum there. Further indicated by the vertical gray mark is the ^{3}He content according to the minimum size from literature data (see Table 1). Reference for all figures displaying data of individual Martian meteorites in this paper: The legend to this figure provides the symbols representing the Martian meteorites and are used in Figs. 2, 3, and 4b as well.

Uranium and Thorium

Thorium and U concentrations (Table 2) were determined by spark source mass spectrometry. About 30–100 mg of powdered meteorite sample was mixed with spiked graphite containing ^{235}U and other spike isotopes, and then pressed into two rod-shaped electrodes. The sample/graphite mixture was analyzed with an AEI-MS 702R mass spectrometer. Uranium concentrations were determined by isotope dilution, thorium concentrations by measuring Th/U ratios, using U for internal standardization and by calibrating with a relative sensitivity factor. Ion detection was performed with a multi-ion counting system (MIC-SSMS; Jochum et al. 2001) consisting of 20 separate channeltrons, except of EETA79001, Lith. B, and LEW 88516, where a photoplate was used. Uncertainties (1 RSD) of the U and Th data are about 5–7%.

Shock Pressure

The most recent comprehensive data set by Fritz et al. (2005a, 2005b) is taken for this study. The work reports on shock pressures of 18 Martian meteorites which cover the whole suite of available Martian lithologies. “Equilibration” shock pressures ranging from 5 to 55 GPa were determined based on the shock metamorphic overprint recorded by rock texture and the rock forming minerals olivine, pyroxene and plagioclase (Stöffler et al. 1986, 1991; Bischoff and Stöffler 1992; Schmitt 2000). Details of the methods which include refractive index measurements on plagioclase/maskelynite and Raman spectroscopy are given in Fritz et al. (2005a, 2005b). The shock pressure calibration based on micro-Raman-spectroscopy was used to determine the degree of shock metamorphic overprint in the lherzolitic shergottite Y-793605, for which only thin sections were available. The results and a comparison to literature data is given in Table A1 in the online data collection.

Shock and Post-shock Temperatures

Post-shock temperatures for Martian meteorites were calculated as in Artemieva and Ivanov (2004) and Fritz et al. (2005a), shock temperatures for pressures <33 GPa with the same equations of state using the method described in Artemieva and Ivanov (2004). Shock temperatures resulting from shock compression >32 GPa were computed with a program written by Schmitt (1995, 2000), and values for olivine, pyroxene (enstatite) and plagioclase (oligoclase) were taken from (Schmitt 1995). A model for calculating the Hugoniot curves of mixed materials (Munson and Schuller 1971) was used to calculate the Hugoniot curves of rocks with according modal compositions. These calculated Hugoniot

Table 2. Database for loss calculations and calculated loss (this study and literature data), U and Th from this study if not stated otherwise, crystallization ages from literature as given in column reference.

Meteorite	U (ppm)	Th (ppm)	Crystallization age	Reference	Loss (%), this study	Loss (%) literature mean[g]	Number of analyses[h]
ALHA77005	0.0062	0.024	179 Ma	1	100 ± 30	94 ± 3	6
ALH 84001	0.016	0.037	4.0 Ga	2	89 ± 9	85 ± 7	15
Chassigny	0.019	0.051	1.34 Ga	1	46 ± 6	21 ± 18	8
DaG 476	0.091	0.012	474 Ma	1	100 ± 50 100 ± 12	97 ± 4	5
Dhofar 019	0.11[a]	0.04[a]	525 Ma	3		88	2
EETA79001 Lith A	0.016	0.067	173 Ma	1	56 ± 9	47 ± 11	8
EETA79001 Lith B	0.037	0.145	173 Ma	1		14 ± 10	3
Governador Valadares	0.037	0.17	1.34 Ga	1	51 ± 5	47 ± 6	3
Lafayette	0.028	0.13	1.32 Ga	1	33 ± 6	27 ± 7	4
LEW 88516	0.011	0.040	178 Ma	1	88 ± 20	87 ± 5	4
Los Angeles	0.12[b]	0.57[b]	165 Ma	1		94 ± 5	3
Nakhla	0.043	0.18	1.27 Ga	1	47 ± 5	46 ± 3	5
NWA 480	0.064[c]	0.215[c]	336 Ma	4		(96)	1
QUE 94201	0.0125	0.050	327 Ma	1	90 ± 29	94 ± 3	5
SaU 005/008/094	0.050	0.012	800 Ma	5	99 ± 4	98 ± 3	8
Shergotty	0.089	0.37	165 Ma	1	71 ± 1	65 ± 13	15
Y-000593	0.055[d]	0.23[d]	1.28 Ga	6		55 ± 15	6
Y-793605	0.0036[e]	0.013[e]	212 Ma	1		81	2
Y-980459	0.006[f]	0.0213[f]	472 Ma	7		(87)	1
Zagami	0.102	0.34	177 Ma	1	36 ± 6	56 ± 18	7

[a]Taylor et al. (2002); [b]Jambon et al. (2002); [c]Barrat et al. (2002); [d]Dreibus et al. (2003); [e]Ebihara et al. (1997); [f]mean of the values compiled by Treiman (2005); [g]mean loss calculated from the data set reported in Schultz and Franke (2004); no error range is given for meteorites for which less than three analyses exist; [h]number of analysis, if not otherwise stated as reported in Schultz and Franke (2004).

1: Nyquist et al. (2001); 2: assumed age of complete resetting, see Nyquist et al. (2001); Treiman (1998); 3: Rb/Sr age from Borg et al. (2001); 4: Rb/Sr by Nyquist et al. (2006); 5: E. Jagoutz, Mainz, personal communication; 6: mean of the values compiled by Treiman (2005); 7: Meyer (2006).

curves were applied to estimate the resulting shock temperatures.

Diffusion Modeling

For the modeling of the fractional ^{4}He loss we must consider diffusion data of phosphates, which are the main carrier of U, Th, and accordingly radiogenic ^{4}He. Unfortunately, no data on whitlockite/merrillite exist, so we must restrict ourselves to consideration of apatite diffusion data. For extraterrestrial apatite, there is only one study by Min et al. (2003) on Acapulco apatite. For 2 diffusion experiments on different grains, the authors obtained indistinguishable linear low temperature (100 °C–300 °C) correlations, yielding an activation energy of Q = 44.2 kcal/mol and a preexponential factor of $D_0/a^2 = 24.1\ s^{-1}$. However, these data are largely consistent with diffusion data on terrestrial apatite. The diffusion parameters yield the diffusion coefficient D according to $D = D_0 \exp(-Q/RT)$, (R: gas constant) and the fractional ^{4}He loss according to $F = 1 - 6\pi^{-2} \sum n^{-2} \exp(-n^2\pi^2 Dt/a^2)$, see also previously published procedures in Trieloff et al. (1994, 1998). As a typical post shock degassing time we chose t = 1000 s, which should approximate characteristic time scales before significant cooling from post-shock temperature occurs in a meteorite-sized body (Min and Reiners 2007).

RESULTS AND DISCUSSION

With combining the above described methods, our study aims to evaluate the history and evolution of the helium budgets of Martian meteorites. In the following discussion we are tracking the helium budget from its beginning in the igneous rock on Mars all the way to the laboratory.

Helium Incorporation on Mars

Radiogenic ^{4}He is the product of ^{235}U, ^{238}U, and ^{232}Th decay. Its amount expected for accumulation since igneous formation can be calculated from the concentrations of U and Th and the crystallization age of the meteorite (Table 2).

Cooling History

Radiogenic helium accumulates in a rock after the rock temperature drops below the closure temperature of helium (Farley 2002), but the ages adopted for our calculations are obtained with methods having higher closure temperatures (e.g., Sm-Nd, see Table 2). However, post igneous cooling happens in the very early history of the Martian meteorites, in which only minor amounts of the radiogenic ^{4}He accumulated. For example, all ^{4}He which accumulated in the first 1 Ma in Shergotty equals to 0.6% of the helium otherwise accumulated in the last 165 Ma. Thus, considering the cooling history of

Table 3. U and Th contents of the phosphates of nakhlites Lafayette, Y-000593/000748, and the orthopyroxenite ALH 84001. Data from literature (Lafayette and Y-000593/000748 from Terada and Sano (2004), ALH 84001 from Terada et al. (2003), for bulk data see Table 4).

	Phosphates				Bulk rocks	
Meteorite	Range U (ppm)	Mean U (ppm)	Range Th (ppm)	Mean Th (ppm)	U (ppm)	Th (ppm)
Lafayette	3–37	12	17–160	49	0.028	0.13
Y-000593/000748	3–63	13	10–290	52	0.055	0.23
ALH 84001	0.8–17.9	3.8	9.7–61.2	27.3	0.016	0.037

Martian meteorites (Treiman 2005; McKay et al. 2006; Mikouchi et al. 1999) shows that differences in the closure temperatures of Sm-Nd and (U-Th)/Helium systems can be neglected in our calculations. However a later thermal event, like fluid activity as observed in ALH 84001 (Kring et al. 1998) and the nakhlites (Treiman 2005) could certainly disturb the helium budget of the lithologies.

Extraneous Helium (Atmospheric, Mantle and Inherited Radiogenic) in Martian Meteorites

Two further possible effects occurring on Mars are incorporation of helium from the Martian atmosphere and helium inherited from precursors of the rocks in hand. Adsorption, implantation by shock metamorphism or any other assimilation mechanism cannot account for the incorporation of detectable amounts of helium, because He constantly escapes the atmosphere of Mars: Its lifetime in the Martian atmosphere is only ~$5^{*}10^{4}$ years (Krasnopolsky et al. 1994), and the concentration as low as (10 ± 6) ppm (Krasnopolsky and Gladstone 2005). As far as inherited He is concerned, it is quite reasonable to assume that Martian meteorites are magmatic rocks, which have lost the radiogenic helium accumulated by any precursor rock. We assume the "memory" to have been reset. Therefore, ^{4}He in Martian meteorites has only two sources: in situ radioactive decay of ^{238,235}U and ^{232}Th and cosmic irradiation during passage from Mars to Earth.

Phosphates as U,Th Carrier Phases

Any discussion of ^{4}He must take into account the distribution of radiogenic ^{4}He between the various minerals. From the U and Th contents of phosphates versus bulk (Table 3) it can be seen that no more than 0.2–0.5% of phosphate is needed to account for the amounts of U and Th found in the bulk meteorites. This can be compared to calculated normative apatite contents (Lodders 1998), which vary between 0.03% (ALH 84001) and 2.6% (EETA79001B). We expect the carrier phase for U and Th to be the phosphates.

For Shergotty, similar calculations of the mass balance result in a considerably higher amount of phosphate needed to explain the U and Th content of the bulk rock: 8.1% phosphate is needed in case of U, 4.5% in case of Th, compared to only 1.4% phosphate present in Shergotty (Lodders 1998). Stöffler et al. (1986) estimate up to 2% phosphate for Shergotty. Nevertheless, leaching results obtained by Chen and Wasserburg (1986) and Dreibus et al. (1996) indicate that also for Shergotty phosphates are the primary carriers of U and Th. The highly variable U and Th contents of individual phosphate grains could be problematic for our mass balance calculations: In Y-000593/000749 Terada and Sano (2004) report 10 single measurements of which 8 show concentrations of U between 3 and 9 ppm; one grain shows 25 ppm and one grain 63 ppm. In addition, phosphates as a minor mineral are not necessarily homogeneously distributed in the rock. Either of these or both might account for the high variability in ^{4}He content measured by different authors on different pieces (Schultz and Franke 2004). U and Th were also analyzed by Min et al. (2004) in phosphates from the Los Angeles shergottite. These authors calculate between 83 and 100% ^{4}He loss from their phosphates.

^{4}He Recoil Injection into Adjacent Silicates

The phosphates as major hosts of U and Th are not necessarily the main host of radiogenic He as well. Phosphates in most Martian meteorites are small crystals of several tens of micrometers in size, from which ^{4}He is lost—or transferred into neighboring phases by alpha recoil ejection—more easily than from larger crystals. Comparing the grain size of phosphates in Martian meteorites (e.g., 20–60 μm in Lafayette and Y-000593, Terada and Sano 2004; 40–100 μm in ALH 84001, Terada et al. 2003; 20–100 μm in Shergotty, Sano et al. 2000; ~100 μm in Los Angeles, Min et al. 2004) with helium retention during α-ejection as function of grain size (see Fig. 6 of Farley 2002) shows that a significant fraction must have been ejected. According to this comparison, redistribution of radiogenic ^{4}He should be the rule rather than the exception in Martian meteorites. This is further indicated as pyroxene mineral separates contain considerably more radiogenic ^{4}He (Table 4; Schwenzer et al. 2007) than expected from the U and Th content found by Chen and Wasserburg (1986). Along the same line are results for radiogenic helium in an HCl-etched sample of Nakhla (Ott et al. 1988; weight loss 15%). Data on helium show an inhomogeneous distribution corresponding to 32% loss of ^{4}He only during etching. As etching should have dissolved the phosphates and affected grain boundaries, this may point to an even more intense redistribution than can be expected from implantation due to α-recoil into neighboring phases

Table 4. Concentration of ^{4}He and ^{3}He for bulk and mineral separates (this study). Concentrations are given in 10^{-8} ccSTP/g, mask = maskelynite, ol = olivine.

Meteorite	^{4}He bulk	^{3}He bulk	^{4}He pyroxene	^{3}He pyroxene	^{4}He other	^{3}He other
ALHA 77005	33 ± 3	7.99 ± 0.63	28 ± 1	6.94 ± 0.92	28.9 ± 1 (ol)	6.39 ± 0.15 (ol)
ALH 84001	327 ± 22	26.6 ± 1.8	269 ± 4	23.3 ± 1		
EETA79001, Lith. A	33 ± 4	0.974 ± 0.121	37 ± 1	1.00 ± 0.02		
Governador Valadares	748 ± 51	18.6 ± 1.3	626 ± 10	21.7 ± 0.5		
Lafayette	763 ± 52	19.8 ± 1.5	817 ± 12	20.6 ± 0.5		
Nakhla	836 ± 57	19.9 ± 1.4	672 ± 5	16.2 ± 0.2	250 ± 10 (ol)	16.1 ± 0.7 (ol)
Shergotty	121 ± 1	3.81 ± 0.16	126 ± 1	4.00 ± 0.22	97 ± 1 (mask)	0.92 ± 0.02 (mask)
Zagami	274 ± 19	4.74 ± 0.34	158 ± 3	4.70 ± 0.16	63 ± 9 (mask)	0.94 ± 0.13 (mask)

alone. A possible driving force for further redistribution of ^{4}He may have been the shock metamorphism (see section Identifying Shock Metamorphism as Cause for Helium Loss).

Chassigny

Among the major minerals present in SNC meteorites olivine is most retentive for helium (Hintenberger et al. 1966, 1967). The dunite Chassigny contains significantly less U and Th than most of the shergottites, but unfortunately no data on the U and Th content of olivine itself exist. Uranium and thorium contents are similarly low in the lherzolitic shergottites (57 ± 3 ppb Th and 15 ± 3 ppb U in ALHA77005; 37 ± 9 ppb Th and 14 ± 7 ppb U in LEW 88516; compared with 57 ppb Th and 18 ± 4 ppb U in Chassigny, all data from Lodders 1998). However, the normative amount of apatite is 0.9% in the lherzolitic shergottites versus only 0.2% in Chassigny, which—given the U and Th concentration in apatites from Chassigny and the shergottites are comparable—requires an additional carrier of U and Th in Chassigny. In fact, while petrological investigations describe Chassigny to contain only traces of phosphates, 0.3% melt inclusions in the olivine host crystals have been reported (Floran et al. 1978). Apatite is present in the multiphase type of these inclusions (Floran et al. 1978; Varela et al. 2000). Thus, these inclusions might contain significant amount of U and Th which is therefore enclosed by the olivine host. Consequently, Chassigny can be expected to show a different behavior in terms of its helium compared to the other Martian meteorites. For that reason, Chassigny will be treated separately in the final discussion of the relation between He loss and shock pressure.

On Mars: Pre-Irradiation and Ejection Events

Cosmic ray exposure produces nuclides amongst which are ^{3}He and ^{4}He. Given the thin atmosphere, 2π-irradiation is possible on Mars. Therefore, the burial depth and excavation history of the rock, which became a meteorite later, is relevant.

During the course of studying the Martian meteorites, the inferred number of cratering events evolved from one source crater (see Treiman 1995 for a detailed literature survey and history) to up to eight different ejection events and, thus, source craters (Eugster et al. 2002; Eugster 2003; Christen et al. 2005; Fritz et al. 2007a). The size frequency distribution of impact ejecta leaving Mars is dominated by small rock fragments with a 4-π cosmic ray geometry (Head et al. 2002; Artemieva and Ivanov 2004). The distribution of the cosmic ray exposure ages of the recovered Martian meteorites shows that these rock fragments were ejected as small bodies from Mars accumulating cosmogenic nuclides immediately after launch, thus range from 0.2 to 2 m in diameter (Eugster et al. 2002).

A near-surface position in principle would allow pre-irradiation on Mars before ejection. For a depth of 10–20 cm below Martian surface and taking the atmosphere into account Eugster (2003) calculated that $(70 \pm 20)^{*}10^{-8}$ ccSTP/gram of ^{3}He is produced in a rock of "average" Martian composition over a time of 100 Ma. This is more by a factor of 2.6 to 72 than measured in our Martian meteorite samples (Table A2). On the other hand, the concordant cosmic ray exposure ages calculated not only from stable noble gas isotopes but also from ^{10}Be and ^{53}Mn, excesses of ^{80}Kr and by the ^{81}Kr-^{83}Kr method, argue against both pre-irradiation and launch as a big object followed by breakup in space (Eugster et al. 2002). Warren (1994) estimated a burial depth of >4 m for the nine Martian meteorites known at the time. Today for only two (Y-793605 and Y-980459) of the currently known 38 unpaired Martian meteorites listed by Meyer (2006, updated online 2008) any hint for possible parent body irradiation has been reported (Nagao et al. 1997; Nishiizumi and Hillegonds 2004). We therefore assume for the course of this study the ^{3}He to be of cosmogenic origin and solely obtained during space travel as small objects.

Identifying Shock Metamorphism as Cause for Helium Loss

Plotting ^{3}He versus ^{4}He (Fig. 2) separates the Martian meteorites in two groups: those falling close to the line of cosmogenic ^{4}He/^{3}He = 4.1 (or alternatively 6.2, also shown) and those showing higher ^{4}He concentrations due to the presence of radiogenic helium. All nakhlites and ALH 84001 fall clearly to the right of even the 6.2 ratio line. For the

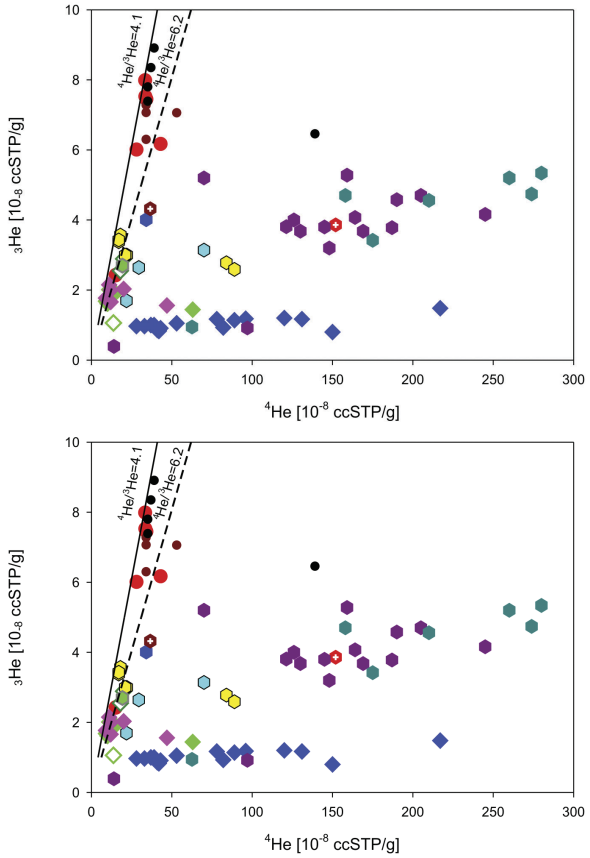

Fig. 2. ^{3}He versus ^{4}He. Literature data: Schultz and Franke (2004), petrological groups of Martian meteorites (after Goodrich 2002) are indicated by shape of symbol as in Fig. 1. The lines indicate possible cosmogenic ratios ^{4}He/^{3}He of 4.1 and 6.2 (our lowest ratio and Welten et al. 2003, respectively).

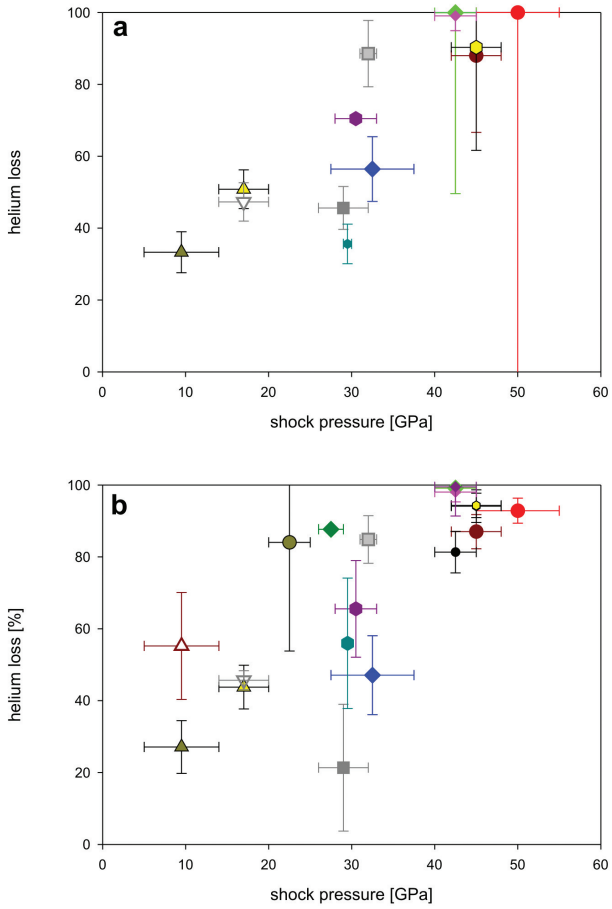

Fig. 3. Helium loss in % versus shock pressure (Table 1; Fritz et al. 2005). Petrological groups of Martian meteorites (after Goodrich 2002) are indicated by shape of symbol as in Fig. 1. Helium loss has been obtained by subtracting the measured radiogenic helium from the expected amount of radiogenic helium based on U and Th concentrations and the crystallization age (see Table 2 and text). The measured radiogenic helium has been calculated from the measured value subtracting cosmogenic ^{4}He calculated from the measured ^{3}He: (a) using He, U and Th data from this study only (Tables 1 and 2); (b): taking all data from the literature (Schultz and Franke 2004); shown are mean value of individual data (as also listed in Table 2). The error range represents the scatter of the data in the compilation (Please note that meteorites for which less than 3 measurements exist are plotted without error range).

chassignites this holds true only for Chassigny itself, but not for NWA 2737. The shergottites in general fall closer to the line, which is—at least in part—a result of their younger crystallization ages and consequently lower radiogenic ^{4}He contents. Differences can also be observed amongst the shergottites: Some (e.g., ALHA77005, QUE 94201, and Y-980593) fall on or close to cosmogenic with all their data points, whereas others (e.g., Zagami and Shergotty) plot clearly to the right. As radiogenic ^{4}He is dependent on crystallization age and Th and U contents, some variation is to be expected, but plotting on or very close to the cosmogenic ratio requires significant loss of radiogenic ^{4}He.

Following up on this observation the deficits of radiogenic ^{4}He were calculated (see section 2.2). The results are given in Table 1 and apparent losses are plotted versus shock pressure in Fig. 3. Our own U, Th, He data (Fig. 3a) obtained on aliquots show a clear correlation of helium loss and shock pressure. Taking all data available (Fig. 3b) results in significant scattering as indicated by the error bars. The differences are most likely due to sample heterogeneity and determination of U, Th, He on different portions of the respective meteorites. However, the overall correlation persists.

In detail, plotting fractional ^{4}He loss versus shock pressure shows 20–50% loss at pressures below 30 GPa, a strong increase in fractional ^{4}He loss around 30 GPa, and almost total loss above 30 GPa. The value of ca. 30 GPa is characteristic for the plagioclase-maskelynite transition. The transformation from plagioclase to maskelynite (or plagioclase glass at higher pressures) dominates the amount of waste heat deposited in these olivine-pyroxene-plagioclase-rich rocks by the passing shock wave (Fig. 4a). At a given pressure plagioclase is shock heated to higher temperatures compared to olivine and pyroxene. Quickly after passage of the shock wave the different minerals equilibrate to the post-shock temperatures calculated for the

bulk rock. This may also affect phosphates, which are the main carrier phase of U, Th but maybe not contain all of the radiogenic ^{4}He (see recoil in section Helium Incorporation on Mars) and are frequently intergrown with plagioclase (e.g., Greenwood et al. 2003).

Quantitative Models for Shock-Induced Diffusion

In order to quantitatively check the retentivity of phosphates under elevated post-shock temperatures, we modeled (see section Diffusion Modeling) the fractional ^{4}He loss using the low temperature diffusion data for Acapulco apatite by Min et al. (2003). Post-shock temperatures of ≥370 °C are needed to cause ≥50% loss, assuming similar grain size as Acapulco apatite and a typical degassing or cooling time of 1000 seconds. It should be mentioned that the effect of grain size is rather minor: reducing the grain size by a factor of two would imply that 50% loss could occur at 350 °C instead of 370 °C, i.e., temperature is the dominant factor controlling diffusional He loss. Besides post-shock temperatures, shock metamorphism offers another potential process capable to induce ^{4}He loss, namely the shock temperature during the passage of the shock wave. Shock temperatures are much higher than post-shock temperatures, but are maintained for a much shorter time, e.g., only a few milliseconds in the case of SNC meteorites. It is, however, nearly impossible to predict how effective He diffusion is in a dynamically compressed mineral, so any consideration about ^{4}He loss caused by this process remains highly speculative. Hence, we will restrict our discussion to post-shock temperature effects in the following.

Figure 4a shows the correlation of post-shock temperature increase and shock pressure for various minerals (olivine, enstatite, oligoclase—data by Schmitt 1995) and rocks (pyroxenite, dunite—after Artemieva and Ivanov 2004, Fritz et al. 2005a). While olivine and pyroxene (and rocks in which these minerals prevail) require very high shock pressures of >60 GPa to reach post-shock temperatures causing 50% ^{4}He loss (370 °C), plagioclase needs only about 30 GPa, a circumstance that can be ascribed to the high compressibility of plagioclase. Unfortunately, for phosphates no equation of state data are available that would allow calculation of respective post-shock temperatures. For Martian meteorites—polymineralic mixtures of these components—a very heterogeneous distribution of post-shock temperatures can be expected immediately after passage of the shock wave, with plagioclase minerals being relatively hotter than olivine or pyroxene minerals. After some time, thermal equilibration in rocks is achieved. Temperatures after thermal equilibration are intermediate between plagioclase and pyroxene/olivine (Fig. 4a) and would require about 40 GPa shock pressure to cause 50% ^{4}He loss.

Post-shock heating effects are quantitatively explored in Fig. 4b displaying the correlation of shock pressure and ^{4}He loss: the first model curve shows the ^{4}He loss assuming that phosphates in each SNC meteorite experience only the bulk equilibration post-shock temperature. This model can only explain high losses at very high pressures, but not significant losses around 30 GPa. The second model assumes that phosphates in each SNC meteorite suffer from similar post-shock temperatures as plagioclase. This model curve yields a surprisingly good fit, not only for >35 GPa samples, but particularly the steep increase for samples shocked around 30 GPa is well reproduced. Only the weakly shocked nakhlites can hardly be explained by post-shock temperature triggered ^{4}He losses.

Admittedly, our model is a simplified approach that considers "equilibration" shock pressures only. As noted above, localized regions can experience pressure-temperature spikes far above the equilibration shock pressure, e.g., due to varying porosity. This can result in heterogeneous post-shock temperature distributions of individual mineral species, causing variably degassed phosphate grains. Another possibility to yield variably degassed phosphate grains is a grain size distribution, as small grains are more susceptible to ^{4}He loss. Indeed, phosphates degassed to very different degrees were identified in a recent U,Th-He dating study by Min and Reiners (2007) in ALH 84001, an observation leading the authors to conclude that the shock (and ejection) event caused variably partial degassing. Finally, carrier phases other than phosphates, e.g., adjacent minerals with recoil implanted ^{4}He, can add significant complexity.

Differential Retentivity of He Carrier Phases

Helium loss is strongly dependent on diffusion properties. Grain size may be expected to have an influence on the extent of loss, but no correlation could be observed between helium loss and grain size of the constituent minerals in the Martian meteorites of this study. As mentioned before, the mineralogical composition of the samples of interest may be more important. Phosphates apatite and merrillite are the main U,Th and ^{4}He carriers, and their retentivity can be considered to be lower than that of other main minerals like plagioclase, olivine or pyroxene (Pellas et al. 1997; Farley 2002; Trieloff et al. 2003). As maskelynite shows significant ^{3}He loss by solar heating (up to 30%, Schwenzer et al. 2007) in SNC meteorites, it would also be expected to experience loss of—recoil ejected ^{4}He. The data set does not allow a clear-cut conclusion as the two individuals with the highest maskelynite content (Los Angeles and QUE 94201) are also having very high helium loss. These belong to the group of meteorites for which ~45 GPa shock pressure are determined (Table A1; Fritz et al. 2005a). Other individuals show similarly high loss in spite of much lower maskelynite content (ALHA77005, DaG 476, LEW 88516, SaU 005). Thus it appears that peak shock pressure rather than maskelynite content is related to loss of radiogenic ^{4}He, although minor effects cannot be excluded. As phosphates are considered to be less retentive than maskelynite, some of their ^{4}He inventory could have been lost by solar radiation, but probably no more than 30%, as in the case of Lafayette (Table 2). Besides the fact that there are no unshocked Martian meteorites, all investigated individuals have lost at

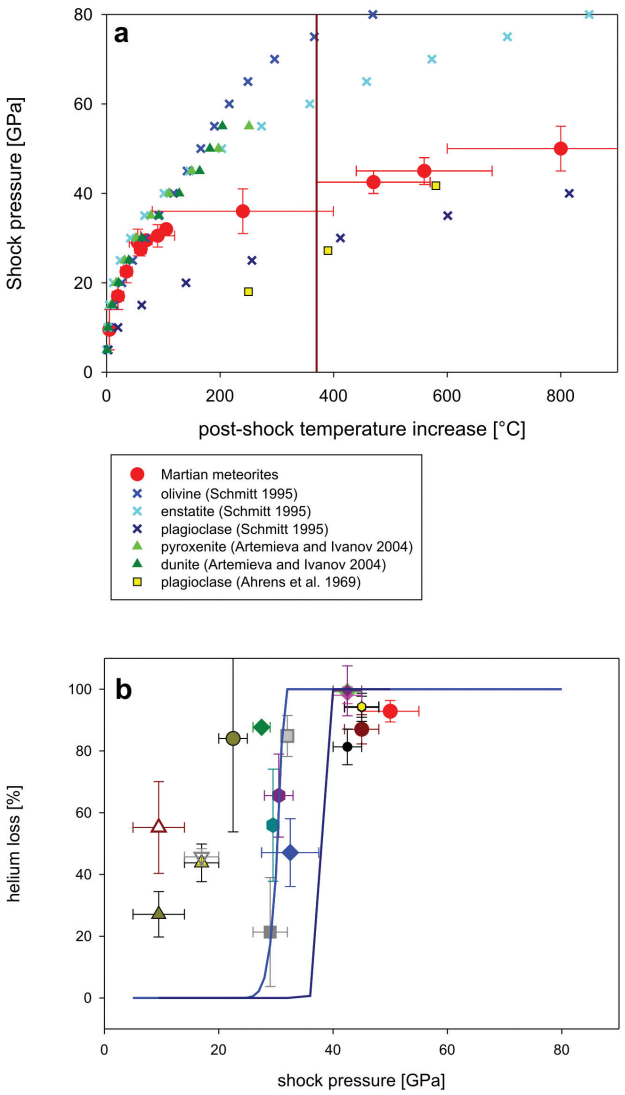

Fig. 4. a) Correlation of shock pressure and post-shock temperature in various minerals (olivine, pyroxene, oligoclase—data from Schmitt 1995) and rocks (pyroxenite, dunite, calculated after Artemieva and Ivanov 2004; Fritz et al. 2005a). Plagioclase displays strongest post-shock temperature increase, olivine and pyroxene weakest. For apatite no data exist. Brown vertical line at 370 °C indicates temperature, at which 50% radiogenic helium is lost from apatite for a heating time of 1000 seconds. b) If apatite experiences similar post-shock temperatures as plagioclase, the correlation of ^{4}He loss and shock pressure of most Martian meteorites can be satisfactorily explained, except for nakhlites, which may have suffered ^{4}He loss by additional effects (e.g., solar heating, see text). Light blue line indicates the fractional He loss assuming the same post shock temperature increase for apatites as for plagioclase, dark blue line is the predicted He loss if apatite experiences only the post shock temperature after thermal equilibration of whole rocks. The better agreement with the blue curve could either indicate that apatite is affected by post shock temperature increase similar to plagioclase, or that local excursions in shock pressure and post shock temperature increase strongly degas a certain fraction of apatite crystals before thermal equilibration of whole rocks is achieved.

least 20% of their radiogenic ^{4}He. This could either be the results of some loss from "high diffusion" phases during space travel, as indicated by the ^{3}He loss (see section ^{3}He and Cosmic-Ray Exposure: The Space Travel), or due to the fact that the same phases form local hot spots during shock metamorphism.

The Role of Shock-Induced Melting for the He Retentivity

Another feature to consider is the presence of shock-produced melt glasses. Melting occurs due to pressure peaks caused by differing physical properties at phase boundaries (Fritz et al. 2005a; Stewart et al. 2007) and is especially pronounced, when open pore space is present (Stöffler et al. 1991; Heider and Kenkmann 2003; Stewart et al. 2007). Melt formation is important here, because melting changes the diffusion parameters of the phases completely. A first anticipation is that melting increases the probability of helium loss, which is not necessarily true. McConville et al. (1988) found that glass, due to the increased diffusion length and activation energy retained substantial amounts of argon in their study. Considering the complete data set on EETA79001, there might be a hint to that fact in the helium contents measured. Lithology A and Lithology B vary internally by about a factor of 2 (which can be accounted as small sample size effect). Lithology C, which is dominated by glass, contains almost as much ^{4}He as lithology A. For the amount of helium in the shock glass that is present as inclusions in the rock, this observation is either due to the effects found by McConville et al. (1988) or can be taken as another argument for redistribution of ^{4}He after the shock event. However, in general, less than 15% of the meteorite mass is converted to shock melt (e.g., Walton and Herd 2007). The highest amounts occur in ALHA77005 (13.7%, Treiman et al. 1994). Given the almost uniform distribution of helium (Table A2), the amount of shock melt should have a detectable influence on the helium loss. Details, however, are masked by the fact that the formation of shock melt requires high shock pressure; therefore these mechanisms cannot be separated.

ALH 84001 and Chassigny

ALH 84001 has experienced multiple overprinting events (Treiman 1998). All of these processes are capable of influencing the helium budget. Disentangling them in detail is beyond the scope of this paper and cannot be done by helium alone. What can be stated from our data is that most likely ALH 84001 lost all its ^{4}He 4 Ga (Nyquist et al. 2001) ago. Then ongoing U and Th decay produced radiogenic helium. Not all of this new ^{4}He is still present. It can be concluded that the event that caused the shock metamorphic overprint and the helium loss observed now was the launching event dated by its cosmic ray exposure age, in agreement with conclusions by Min and Reiners (2007).

Chassigny is the individual showing the smallest amount of He-loss although its shock metamorphic overprint (26–32 GPa) is significantly higher than that of the nakhlites and was subjected to similar shock pressure as some shergottites. Note that in these shergottites all plagioclase was transformed to maskelynite, while the more Na-rich plagioclase in Chassigny is present as birefringent and partly isotropic plagioclase. Only some plagioclase grains in Chassigny were transformed to maskelynite (Fritz et al. 2005a, 2005b). The different plagioclase chemistry and the high retentivity of olivine may explain the comparably small amount of helium loss in Chassigny.

^{3}He and Cosmic Ray Exposure: The Space Travel

The amount of radiogenic ^{4}He was calculated using the of $(^4He/^3He)_{cosm}$ which implies that all cosmic ^{3}He is preserved in the meteorite. To verify these arguments the possibility of helium loss during space residence time has to be discussed.

^{3}He and Cosmic Ray Exposure Ages

^{3}He is almost exclusively of cosmogenic origin, therefore its abundance depends primarily on the exposure age, geometry (shielding) and the chemistry of the target meteorite. Effects that could cause loss of ^{3}He include solar heating but also loss due to weathering. Loss may also have occurred as loss of ^{3}H, which is a precursor for part of ^{3}He (Leya et al. 2004) and diffuses much easier, at least in metals (Hintenberger et al. 1966, 1967).

Comparing the ^{3}He budgets of Martian meteorites reveals no systematic differences between the ^{3}He (and ^{4}He) amounts observed in falls and finds (hot desert, cold desert, other), but shows differences obviously related to the differences in cosmic ray exposure ages (Fig. 1). Comparing the ^{3}He content—or, alternatively, exposure ages obtained from this isotope alone—with cosmic ray exposure ages calculated from cosmogenic nuclides different from ^{3}He (Table 1) reveals a fair correlation between those CRE ages and measured ^{3}He. This indicates the cosmogenic origin of ^{3}He and subsequent preservation without significant losses.

In detail, of course, production of cosmogenic helium depends on target chemistry and shielding (see details in section Helium and Table 1). The observed ^{3}He concentrations can be explained as a function of the meteorites' chemistry combined with their exposure ages (Fig. 1). No ^{3}He loss is needed to explain the data set, but, of course, it is also impossible to completely rule out minor losses. The only exception is Los Angeles, which is a desert find with cloudy history and unknown terrestrial age. Two possible explanations come to mind: a very large radius (r > 40 cm) or terrestrial influence. Another interesting case is Dhofar 019 for which Shukolyukov et al. (2002) suggested that ^{3}He was lost as a result of solar heating or weathering. There are several assumptions concerning the minimum radius: 4.2 cm (the minimum radius from our data set, Table 1), >7 cm (Nishiizumi et al. 2002), 15–20 cm (Shukolyukov et al. 2002). In addition, there are three estimates for the age: 18.1 Ma (Shukolyukov et al. 2000), 18.7 ± 4.3 Ma (^{21}Ne only, Nishiizumi et al. 2002) and 20 Ma (Shukolyukov et al. 2002, Park et al. 2001). Depending on which data are used to compute the ^{3}He with the model of Leya et al. (2000) and the age, the ^{3}He is what is expected within error or shows loss up to a maximum of 30%.

^{3}He and ^{21}Ne

The discussion above that focuses on ^{3}He production alone ignores the fact that by changing the geometrical parameters (meteoroid size and specimen depth) also the production rate of the other cosmogenic nuclides and hence the inferred exposure age will change (an exception is the ^{81}Kr-Kr system). A more sensitive method to evaluate changes to the cosmogenic ^{3}He budget of a meteorite is plotting $(^3He/^{21}Ne)_c$ versus $(^{22}Ne/^{21}Ne)_c$ ("Bern-Plot", Eberhardt et al. 1966). Two processes can account for a shift away from the correlation line: solar cosmic irradiation will shift $(^{22}Ne/^{21}Ne)_c$ ratios to higher values than expected from pure galactic cosmic irradiation, while loss of ^{3}He will lower the $(^3He/^{21}Ne)_c$ ratio, thus shift down the data points parallel to the ordinate. Theoretical neon isotopic ratios as well as the $(^3He/^{21}Ne)_{GCR}$ ratios can be calculated using the production rates given by Leya et al. (2000). Making detailed considerations that also take the chemistry of the irradiated object in account results in a very good agreement between the theoretically calculated Leya-line(s) and measured data for the nakhlites, and the chassignites. A fairly good fit also is seen for ALH 84001 and the lherzolitic shergottites. The shergottites in general show some variation that can be related to solar cosmic ray contribution as has been described previously (Garrison et al. 2005; Schwenzer et al. 2007). The greatest deviation from the theoretical values is observed in the basaltic shergottites. It can be accounted to variation in chemistry as well as solar cosmic irradiation. These observations agree with what has been noted by independent previous studies: calculated ejection ages determined using empirical relations for production rates of cosmogenic He (T_3), Ne (T_{21}), and Ar (T_{38}) are not systematically lower for T_3 in comparison with T_{21} and T_{38} (see Eugster et al. 1997; Schwenzer 2004).

Obviously major loss of cosmogenic helium from most of the bulk Martian meteorites due to near solar heating did not occur. This is further supported by studies on the orbital parameters of Earth reaching Martian meteoroids (Gladman et al. 1996; Gladman 1997).

Influence of Terrestrial Weathering

As most of the Martian meteorites are finds, quantifying or at least estimating the terrestrial influence is one key parameter. Weathering in general acts on grain boundaries, therefore surfaces exposed due to fracturing and small grains are more easily affected. As a consequence nuclides—such as radiogenic ^{4}He—sited in such positions due to recoil implantation or size

of their host minerals will be more easily lost than elements distributed homogeneously in the main minerals.

To explore the effects of weathering, the L6 chondrite Holbrook is a unique sample, as specimens of it have been collected shortly after the fall in 1912, then 19 years later in 1931 and another 37 years later in 1968 (Gibson and Bogard 1978). Decrease in ^{3}He as well as, but less pronounced, in ^{4}He is observed especially for the first period of exposure to terrestrial influence. Further, the ^{3}He/^{21}Ne ratio is described to change "erratically" (Gibson and Bogard 1978). Other studies on weathered chondrites (Scherer et al. 1994) found loss of radiogenic helium as well as cosmogenic helium, neon and argon. In their study of a large number of H chondrites, based on abundance of radiogenic ^{40}Ar and the ratio of exposure ages calculated via ^{38}Ar and ^{21}Ne, Graf and Marti (1995) identified a number of cases with evidence for noble gas loss due to weathering. Furthermore, according to Alexeev (1998) non-Antarctic finds have (16 ± 4)% less ^{4}He on average compared to falls, whereas Antarctic finds have only (5 ± 3)% less. Finally, the average nominal cosmic ray exposure age of non Antarctic H chondrite finds belonging to the ~7 Ma exposure peak is about 15% lower than that of falls, for which terrestrial weathering is the most likely reason (Alexeev 2005). Laboratory experiments simulating the effect of rainwater on enstatite chondrites, however, have not supported these results so far for cosmogenic He and Ne (Patzer and Schultz 2001), while, on the other hand, significant losses of cosmogenic Ar were observed.

As for ^{3}He in Martian meteorites, terrestrial weathering is a possible explanation for the low ^{3}He abundance of Los Angeles. Similarly, low concentrations observed in some other cases may be a result of unintended sampling of weathered portions of the meteorites. The observation of reduced ^{3}He amounts in weathered samples might not only be caused by loss of ^{3}He from meteoritic mineral grains, but also could occur due to dilution of the analyzed sample by terrestrial material.

As for ^{4}He, terrestrial weathering can also contribute to the low observed helium concentrations to some extent by loss or dilution. There are two individuals in our data set, DaG 476 and SaU 005, described as heavily weathered (Dreibus et al. 2000; Zipfel 2000). Unfortunately, they belong to the group with shock pressures >40 GPa and thus are expected to have lost all their radiogenic ^{4}He due to shock already. Therefore, no direct evidence for weathering influence can be seen. The only observation that clearly argues against significant loss due to weathering, is the fact that—as discussed for ^{3}He—the contents of cosmogenic helium fit to the expected ranges calculated from the theoretical production rates (Fig. 1) and ^{3}He/^{21}Ne ratios.

With respect to weathering, it is useful to turn to the nakhlites as example: There is an Antarctic find (Y-000593), a most likely find (Lafayette) with comparably long terrestrial age, an individual most likely collected shortly after the fall (Governador Valadares) and an observed fall (Nakhla). The observations possible on the nakhlites (see Figs. 1, 2, 3, 5b, and Table A1) argue against major influence from weathering. This leaves shock metamorphism as the major cause for the observed loss of radiogenic helium.

CONCLUSIONS

In our study, we investigated the budgets of ^{3}He and ^{4}He in Martian meteorites. The—purely cosmogenic—^{3}He is used as a measure for processes influencing the helium budget after the meteorites' launch from Mars. From considering the budgets of ^{3}He and ^{21}Ne, we exclude significant influence of solar heating and terrestrial weathering on the main minerals hosting cosmogenic helium (olivine, pyroxene). Exceptions are the meteorites with high maskelynite content as maskelynite shows indication for minor ^{3}He loss (Schwenzer et al. 2007). Consequently, observed deficits of radiogenic ^{4}He in bulk Martian meteorites via solar heating are only possible if ^{4}He bearing phases are affected selectively. This appears possible in principle, as phosphates are the main carrier of U, Th and radiogenic ^{4}He, and have a low helium retentivity. However, major minerals like olivine and pyroxene can host significant amounts of ^{4}He, which was implanted by α-recoil ejection from adjacent phosphates. These more retentive minerals would not be susceptible to solar heating loss. Moreover, solar heating can hardly explain the correlation of ^{4}He loss and shock pressure presented here, nor the fact that the degassing degree strongly varies within individual phosphates (Min and Reiners 2007). This is the key argument that ^{4}He loss is directly related to shock metamorphism.

Nevertheless, other loss mechanisms than shock metamorphism may play a minor role: No meteorite has kept all its radiogenic helium. Particularly for the minimum loss of ~30% for the weakly shocked nakhlites alternative explanations appear possible: Solar heating selectively affecting ^{4}He in phosphates, or diffusional loss during the meteorites' pre-shock history, e.g., during slow cooling or temperature excursions during residence in the Martian crust (Treiman 2005; Mikouchi et al. 2006). Moreover, the nakhlites show alteration minerals formed on Mars (Treiman 2005). Given the timing and expected temperatures of these events, we assume the event that formed the secondary minerals to be the most likely cause for this ~30% loss (cf. sections Helium Incorporation on Mars [cooling history] and ^{3}He and Cosmic Ray Exposure: The Space Travel [solar heating]).

Our study on naturally shocked Martian meteorites confirms a causal relationship of shock metamorphism and He loss. Hence, a comparison of U/Th-He and crystallization ages can give a rough estimate of the shock pressure experienced by Martian meteorites. Further experimental investigations related to the retentivity of ^{4}He during shock metamorphism are mandatory to more definitely evaluate the influences of shock temperature during shock wave passage

and post-shock temperature afterwards. We also note that shock has been shown to lead to loss from other noble gas carriers like phase Q, the main carrier of trapped noble gases in chondrites (Nakamura et al. 1997).

From a more general perspective, retention of helium during shock compression has also significant implications for the concentration of ^{3}He in the solar wind enriched regolith on the impact gardened surface of the Moon. In turn, the magnitude of impact induced ^{3}He loss from regolith material will influence the ^{3}He concentration of lunar impact ejecta delivered to Earth and their contribution to the volume of ^{3}He measured in Earth's sediments (Fritz et al. 2007b).

Below we summarize sequentially the various events that may have influenced the budget of radiogenic ^{4}He.

1. Formation of rock, cooling, and start of He retention: a significant time lag between formation and reaching the closure temperature may cause a ^{4}He deficit, especially in the subvolcanic and plutonic rocks.
2. Aqueous alteration on Mars: Th, U, and their host mineral (the phosphates apatite and merrillite) are easily affected by weathering and/or aqueous alteration (e.g., Dreibus et al. 1996; Stopar et al. 2007). For example, the aqueous alteration recorded by iddingsite <700 Ma ago (Swindle et al. 2000) may also have affected phosphates. This effect may be reduced if a significant part of radiogenic He is ejected from phosphates into adjacent phases, if these are less susceptible to weathering. Martian alteration in the nakhlites is confirmed by petrologic investigation (Treiman 2005) and has been speculated to be the reason for fractionated elemental ratios of Kr/Xe (Schwenzer et al. 2006). However, to distinguish between low shock pressure and (mild) alteration as cause for the helium loss, an unshocked Martian rock, i.e., a rock measured on Mars directly or returned from Mars by a sample return mission, would be the key.
3. Shock and ejection from Mars: the observed correlation between shock pressure and He loss (Figs. 3 and 4) demonstrates that shock has been the main process causing loss of radiogenic He. As the nakhlites are subvolcanic rocks and show Martian alteration, processes listed under (1) or (2) may have led to minor losses of their radiogenic helium, which enhances the loss observed at comparably low shock pressures.
4. Solar heating: Since maskelynite has lost a significant part of its cosmogenic ^{3}He, minor loss of radiogenic ^{4}He from apatite with a closure temperature <100 °C during cosmic ray exposure appears feasible. However, a loss of 30% seems to be an upper limit caused by solar heating, as this is the value for Lafayette, belonging to the group with the highest cosmic ray exposure age (10–15 Ma), i.e., with the longest exposure to solar heating effects. Taking 30% loss as an upper limit for helium loss due to solar heating requires this effect to be the only one acting on nakhlites. As other mechanisms most likely contributed to the observed helium loss, we assume the effect to be much smaller if not minor at all.
5. Weathering on Earth: there is little indication for loss of cosmogenic gases from major minerals, particularly olivine which is highly susceptible to weathering. Hence, the influence of terrestrial weathering is likely negligible. As our main conclusion, we confirm the launching event to be the principal event responsible for loss of radiogenic helium. Our results agree with the conclusion of Shuster and Weiss (2005) that the Martian surface temperatures in the history of Mars have been low and therefore helium has been preserved in most of the Martian meteorites. For the nakhlites, however, we observe loss in excess to what is expected from shock metamorphic overprint only. Whether this is caused by the secondary overprint documented by alteration minerals (Treiman 2005) alone or also due to the thermal history of Mars' surface cannot be decided from our helium data alone and requires further study and incorporation of other (noble gas) systems.

Acknowledgments–We want to especially thank David A. Kring and Ludolf Schultz for helpful and encouraging discussions. Thanks to Allan H. Treiman for providing the best estimate of the bulk rock chemistry of Lafayette. Ingo Leya helped us with his spreadsheets for the calculation of cosmic ray production rates. Thoughtful reviews of and pointed suggestions to an earlier version of the manuscript by Don Bogard and Tim Swindle improved the strength of our argumentation. Reviews by Erin Walton and an anonymous colleague and the efficient handling of the manuscript by Tim Swindle are appreciated. We are grateful to the Johnson Space Center (Houston, Texas) and the Museum of Natural History (London) for providing samples. We acknowledge the support by the German Science Foundation (grants Jo305-1/1, Ot 171/3-4, GR-1658) and for J. F. by the Saalbau-HP Weltraumprojekt. Lunar and Planetary Institute Contribution no. 1361.

Editorial Handling—Dr. Timothy Swindle

REFERENCES

Ahrens T. J., Petersen C. F., and Rosenberg J. T. 1969. Shock compression of feldspars. *Journal of Geophysical Research* 74: 2727–2746.

Alexeev V. A. 1998. Parent bodies of L and H chondrites: Times of catastrophic events. *Meteoritics & Planetary Science* 33:145–152.

Alexeev V. A. 2005. The history of ordinary chondrites from the data on stable isotopes of noble gases (a review). *Solar System Research* 39:124–149.

Artemieva N. and Ivanov B. A. 2004. Launch of Martian meteorites in oblique impacts. *Icarus* 171:84–101.

Barrat J. A., Gillet Ph., Sautter V., Jambon A., Javoy M., Göpel C., Lesourd M., Keller F., and Petit E. 2002. Petrology and chemistry of the basaltic shergottite Northwest Africa 480. *Meteoritics & Planetary Science* 37:487–499.

Bastian T. 2004. Radiochemische Analyse langlebiger kosmogener Radionuklide in Marsmeteoriten und Chondriten: Wirkungquerschnitte, Produktionsraten und Modellrechnungen. Ph.D. thesis, University of Cologne, Germany.

Beech M., Nie W., and Coulson I. M. 2007. The Chassigny meteorite fall: A forensic study. *Journal of the Royal Astronomical Society of Canada* 101:139–145.

Beech M., Nie W., and Coulson I. M. 2008. The pre-atmospheric size of the Martian meteorite ALH 77005 progenitor. *Planetary and Space Science* 56:320–325.

Beck P., Gillet P., Barrat J. A., Jambon A., and El Goresy A. 2002. High–pressure silicates in Martian meteorites (abstract). *Geochimica et Cosmochimica Acta* 66:A59.

Beck P., Barrat J. A., Gillet Ph., Wadhwa M., Franchi I. A., Greenwood R. C., Bohn M., Cotten J., van de Moortèle B., and Reynard B. 2006. Petrography and geochemistry of the chassignite Northwest Africa 2737 (NWA 2737). *Geochimica et Cosmochimica Acta* 70:2127–2139.

Bhandari N., Goswami J. N., Jha R., Sengupta D., and Shukla P. N. 1986. Cosmogenic effects in shergottites. *Geochimica et Cosmochimica Acta* 50:1023–1030.

Bischoff A. and Stöffler D. 1992. Shock metamorphism as a fundamental process in the evolution of planetary bodies: Information from meteorites. *European Journal of Mineralogy* 4: 707–755.

Bischoff A., Rubin A. E., Keil K., and Stöffler D. 1983. Lithification of gas-rich chondrite regolith breccias by grain boundary and localized shock melting. *Earth and Planetary Science Letters* 66: 1–10.

Boctor N. Z., Meyer H. O. A., and Kullerud G. 1976. Lafayette meteorite: Petrology and opaque mineralogy. *Earth and Planetary Science Letters* 32:69–76.

Bogard D. D. and Hirsch W. C. 1980. $^{40}Ar/^{39}Ar$ dating, Ar diffusion properties, and cooling rate determinations of severely shocked chondrites. *Geochimica et Cosmochimica Acta* 44:1667–1682.

Bogard D.D., Nyquist L. E., and Johnson P. 1984. Noble gas contents of shergottites and implications for the Martian origin of SNC meteorites. *Geochimica et Cosmochimica Acta* 48:1723–1739.

Bogard D. D., Hörz F., and Johnson P. 1986. Shock-implanted noble gases: An experimental study with implications for the origin of Martian gases in shergottite meteorites. Proceedings, 17th Lunar Planetary Science Conference. pp. 99–114.

Bogard D. D., Hörz F., and Johnson P. 1989. Shock-implanted noble gases II: Additional experimental studies and recognition in naturally shocked terrestrial materials. *Meteoritics & Planetary Science* 24:113–123.

Borg L. E., Nyquist, L.E., Reese Y., Wiesmann H., Shih C.-Y., Ivanova M., Nazarov M.A., and Taylor L. A. 2001. The age of Dhofar 019 and its relationship to the other Martian meteorites (abstract #1144). 32nd Lunar and Planetary Science Conference. CD-ROM.

Chen J. H. and Wasserburg G. J. 1986. Formation ages and evolution of Shergotty and its parent planet from U-Th-Pb systematics. *Geochimica et Cosmochimica Acta* 50:955–968.

Chen M., Sharp T. G., El Goresy A., Wopenka B., and Xie X. 1996. The majorite-pyrope + magnesiowüstite assemblage: Constraints on the history of shock veins in chondrites. *Science* 271:1570–1573.

Christen F., Eugster O., and Busemann H. 2005. Mars ejection times and neutron capture effects of the nakhlites Y-000593 and Y000749, the olivine-phyric shergottite Y-980459, and the lherzolitic NWA 1950. *Antarctic Meteorite Research* 18:117–132.

Dodd R. T. and Jarosewich E. 1979. Incipient melting and shock classification of L-group chondrites. *Earth and Planetary Science Letters* 44:335–340.

Dreibus G., Huisl W., Spettel B., and Haubold R. 2003. Comparison of the chemistry of Y-000593 and Y-000749 with other nakhlites. (abstract #1586). 34th Lunar and Planetary Science Conference. CD-ROM.

Dreibus G., Jagoutz E., Spettel B., and Wänke H. 1996. Phosphate-mobilization on Mars? Implication from leach experiments on SNCs (abstract). 27th Lunar and Planetary Science Conference. pp. 323–324.

Dreibus G., Spettel B., Haubold R., Jochum K.-P., Palme H., Wolf D., and Zipfel J. 2000. Chemistry of a new shergottite: Sayh al Uhaymir 005 (abstract). *Meteoritics & Planetary Science* 35: A49.

Eberhardt P., Eugster O., Geiss J., and Marti K. 1966. Rare gas measurements in 30 stone meteorites. *Zeitschrift für Naturforschung* 21a:414–426.

Ebihara M., Kong P., and Shinotsuka K. 1997. Chemical composition of Y-793605, a Martian lherzolite. *Antarctic Meteorite Research* 10:83–94.

El Goresy A., Chen M., Gillet Ph., and Dubrovinsky L. S. 2000. Shock-induced high-pressure phase transition of labradorite to hollandite "(Na_{47}-Ca_{51}-K_2)" in Zagami and the assemblage hollandite "(Na_{80}-Ca_{12}-K_8)" + jadeite in L chondrites: Constraints to peak shock pressures (abstract). *Meteoritics & Planetary Science* 35:A51.

El Goresy A., Graup G., and Chen M. 2003. The assemblage maskelynite-post-stishovite silica polymorphs in the Shergotty meteorite: New stringent constraints to peak-shock pressures (abstract). *Meteoritics & Planetary Science* 38:A50.

Eugster O. 1988. Cosmic-ray production rates for ^{3}He, ^{21}Ne, ^{38}Ar, ^{83}Kr, and ^{126}Xe in chondrites based on ^{81}Kr-Kr exposure ages. *Geochimica et Cosmochimica Acta* 52:1649–1662.

Eugster O. 2003. Cosmic-ray exposure ages of meteorites and lunar rocks and their significance. *Chemie der Erde* 63:3–30.

Eugster O., Busemann H., Lorenzetti S., and Terribilini D. 2002. Ejection ages from krypton-81-krypton-83 dating and pre-atmospheric sizes of Martian meteorites. *Meteoritics & Planetary Science* 37:1345–1360.

Eugster O., Michel Th., Niedermann S., Wang D., and Yi W. 1993. The record of cosmogenic, radiogenic, fissiogenic, and trapped noble gases in recently recovered Chinese and other chondrites. *Geochimica et Cosmochimica Acta* 57:1115–1142.

Eugster O., Weigel A., and Polnau E. 1997. Ejection times of Martian meteorites. *Geochimica et Cosmochimica Acta* 61:2749–2757.

Farley K. A. 2002. (U-Th)/He dating: techniques, calibrations, and applications. In *Noble gases in geochemistry and cosmochemistry*, edited by Porcelli D., Ballentine C. J., and Wieler R. Reviews in Mineralogy and Geochemistry, vol. 47. Washington, D.C.: Mineralogical Society of America. pp. 819–844.

Floran R. J., Prinz M., Hlava P. F., Keil K., Nehru C. E., and Hinthorne J. R. 1978. The Chassigny meteorite: A cumulate dunite with hydrous amphibole-bearing melt inclusions. *Geochimica et Cosmochimica Acta* 42:1213–1229.

Fritz J., Artemieva N. A., and Greshake A. 2005a. Ejection of Martian meteorites. *Meteoritics & Planetary Science* 40:1393–1411.

Fritz J., Greshake A., and Stöffler D. 2005b. Micro-Raman spectroscopy of plagioclase and maskelynite in Martian meteorites: Evidence of progressive shock metamorphism. *Antarctic Meteorite Research* 18:96–116.

Fritz J., Greshake A., and Stöffler D. 2007a. The Martian meteorite paradox: Climatic influence on impact ejection from Mars? *Earth and Planetary Science Letters* 256:55–60.

Fritz J., Tagle R., and Artemieva N. A. 2007b. Lunar helium-3 in marine sediments: Implication for a late Eocene asteroid shower. *Icarus* 189:591–594.

Garrison D. H., Rao M. N., and Bogard D. D. 1995. Solar-proton-produced neon in shergottite meteorites and implications for their origin. *Meteoritics* 30:738–747.

Gibson E. K. Jr. and Bogard D. D. 1978. Chemical alterations of the Holbrook chondrite resulting from terrestrial weathering. *Meteoritics* 13:277–289.

Gladman B. 1997. Destination: Earth. Martian meteorite delivery. *Icarus* 130:228–246.

Gladman B. J., Burns J. A., Duncan M., Lee P., and Levison H. F. 1996. The exchange of impact ejecta between terrestrial planets. *Science* 271:1387–1392.

Goodrich C. A. 2002. Olivine-phyric Martian basalts: A new type of shergottite. *Meteoritics & Planetary Science* 37:B31–B34.

Graf T. and Marti K. 1995. Collisional history of the H chondrites. *Journal of Geophysical Research* E 100:21,247–21,263.

Greenwood J. P., Blake R. E., and Coath C. D. 2003. Ion microprobe measurements of $^{18}O/^{16}O$ ratios of phosphate minerals in the Martian meteorites ALH 84001 and Los Angeles. *Geochimica et Cosmochimica Acta* 67:2289–2298.

Head J. N., Melosh H. J., and Ivanov B. A. 2002. Martian meteorite launch: High-speed ejecta from small craters. *Science* 298:1752–1756.

Heymann D. 1967. On the origin of hypersthene chondrites: Ages and shock effects of black chondrites. *Icarus* 6:189–221.

Heider N. and Kenkmann T. 2003. Numerical simulation of temperature effects at fissures due to shock loading. *Meteoritics & Planetary Science* 38:1451–1460.

Hintenberger H., Schultz L., and Wänke H. 1966. Messung der Diffusionsverluste von radiogenen und spallogenen Edelgasen in Steinmeteoriten II. *Zeitschrift für Naturforschung* 21a:1147–1159.

Hintenberger H., Schultz L., Wänke H., and Weber H. 1967. Helium- und Neonisotope in Eisenmeteoriten und der Tritiumverlust in Hexaedriten. *Zeitschrift für Naturforschung* 22a:780–787.

Jambon A., Barrat J. A., Sautter V., Gillet Ph., Göpel C., Javoy M., Joron J. L., and Lesourd M. 2002. The basaltic shergottite Northwest Africa 856: Petrology and chemistry. *Meteoritics & Planetary Science* 37:1147–1164.

Jochum K. P., Stoll B., Pfänder J. A., Seufert M., Flanz M., Maissenbacher P., Hofmann M., and Hofmann A. W. 2001. Progress in multi-ion counting spark-source mass spectrometry (MIC-SSMS) for the analysis of geological samples. *Fresenius Journal of Analytical Chemistry* 370:647–653.

Kirsten T., Krankowsky D., and Zähringer J. 1963. Edelgas- und Kalium-Bestimmungen an einer größeren Zahl von Steinmeteoriten. *Geochimica et Cosmochimica Acta* 27:13–42.

Krasnopolsky V. A. and Gladstone G. R. 2005. Helium on Mars and Venus: EUVE observations and modeling. *Icarus* 176:395–407.

Krasnopolsky V. A., Bowyer S., Chakrabarti S., Gladstone G. R., and McDonald J. S. 1994. First measurement of helium on Mars: Implications for the problem of radiogenic gases on the terrestrial planets. *Icarus* 109:337–351.

Kring D. A., Swindle T. D., Gleason J. D., and Grier J. A. 1998. Formation and relative ages of maskelynite and carbonate in ALH 84001. *Geochimica et Cosmochimica Acta* 62:2155–2166.

Leya I., Lange H.-J., Neumann S., Wieler R., and Michel R. 2000. The production of cosmogenic nuclides in stony meteoroids by galactic cosmic-ray particles. *Meteoritics & Planetary Science* 35:259–286.

Leya I., Begemann F., Weber H. W., Wieler R., and Michel R. 2004. Simulation of the interaction of galactic cosmic ray protons with meteoroids: On the production of ^{3}H and light noble gas isotopes in an isotropically irradiated thick gabbro and iron targets. *Geochimica et Cosmochimica Acta* 39:367–386.

Lodders K. 1998. A survey of shergottite, nakhlite and chassigny meteorites whole-rock compositions (abstract). *Meteoritics & Planetary Science* 33:A183–A190.

Loeken Th., Scherer P., Weber H. W., and Schultz L. 1992. Noble gases in eighteen stone meteorites. *Chemie der Erde* 52:249–259.

Marty B., Marti K., and Th. Monod Consortium 2001. Noble gases in new SNC meteorites NWA 817 and NWA 480 (abstract). *Meteoritics & Planetary Science* 36:A122–123.

Marty B., Heber V. S., Grimberg A., Wieler R., and Barrat J.-A. 2006. Noble gases in the Martian meteorite Northwest Africa 2737: A new chassignite signature. *Meteoritics & Planetary Science* 41: 739–748.

McConville P., Kelley S., and Turner G. 1988. Laser probe ^{40}Ar-^{39}Ar studies of the Peace River shocked L6 chondrite. *Geochimica et Cosmochimica Acta* 52:2487–2499.

McKay G., Mikouchi T., and Schwandt C. 2006. Additional complexities in nakhlite pyroxenes: A progress (?) report (abstract #2435). 37th Lunar and Planetary Science Conference. CD-ROM.

Meyer C. 2006. Mars Meteorite Compendium. http://curator.jsc.nasa.gov/antmet/mmc/index.cfm. Last accessed November 2008.

Mikouchi T., Miyamoto M., and McKay G. A. 1999. Cooling rates of olivine in the Martian meteorites Dar al Gani 476 and Elephant Moraine 79001 (abstract). *Meteoritics & Planetary Science* 34: A81–A82.

Mikouchi T., Miyamoto M., Koizumi E., Makishima J., and McKay G. A. 2006. Relative burial depths of nakhlites: An update (abstract #1865). 37th Lunar and Planetary Science Conference. CD-ROM.

Min K. and Reiners P. W. 2007. High-temperature Mars-to-Earth transfer of meteorite ALH 84001. *Earth and Planetary Sciences Letters* 260:72–85.

Min K., Farley K. A., Renne P. R., and Marti K. 2003. Single grain (U-Th)/He ages from phosphates in Acapulco meteorite and implications for thermal history. *Earth and Planetary Science Letters* 209:323–336.

Min K., Reiners P. W., Nicolescu S., and Greenwood J. P. 2004. Age and temperature of shock metamorphism of Martian meteorite Los Angeles from (U-Th)/He thermochronometry. *Geology* 32: 677–680.

Munson D. E. and Schuller K. W. 1971. Hugoniot predictions for mechanical mixtures using effective moduli. In *Shock waves and the mechanical properties of solids*, edited by Burke J. J. and Weiss V. Syracuse: Syracuse University Press. pp. 185–202.

Nagao K. 1987. Rare gas isotopic composition of achondrites from Antarctica. *Proceedings of the Twelfth Symposium on Antarctic Meteorites*. pp. 110–111.

Nagao K. and Matsuda J. 1986. Rare gas studies of Antarctic Meteorites. *Proceedings of the Eleventh Symposium on Antarctic Meteorites*. pp. 131–132.

Nagao K., Nakamura T., Miura Y. N., and Takaoka N. 1997. Noble gases and mineralogy of primary igneous materials of the Y-793605 shergottite. *Antarctic Meteorite Research* 10: 125–142.

Nakamura T., Zolensky M. E., Hörz F., Takaoka N., and Nagao K. 1996. Shock effects on phase Q and HL diamonds inferred from experimental shock loading on Allende meteorite. 28th Lunar and Planetary Science Conference. pp. 1001–1002.

Nishiizumi K., Caffee M. W., Jull A. J. T., and Klandrud S. E. 2001.

Exposure history of shergottites Dar al Gani 476/489/670/735 and Sayh al Uhaymir 005 (abstract #2117). 32nd Lunar and Planetary Science Conference. CD-ROM.

Nishiizumi K., Caffee M. W., and Masarik J. 2000. Cosmogenic radionuclides in the Los Angeles Martian meteorite. *Meteoritics & Planetary Science* 35:A120.

Nishiizumi K. and Hillegonds D. J. 2004. Exposure and terrestrial histories of new Yamato, lunar, and Martian meteorites. *Antarctic Meteorites* 28:60–61.

Nishiizumi K., Okazaki R., Park J., Nagao K., Masarik J., and Finkel R. C. 2002. Exposure and terrestrial histories of Dhofar 019 Martian meteorite (abstract #1366). 33rd Lunar and Planetary Science Conference. CD-ROM.

Nyquist L. E., Shih C.-Y., Reese Y. D. and Irving A. J. 2006. Concordant Rb-Sr and Sm-Nd ages for NWA 1460: A 340 Ma old basaltic shergottite related to lherzolitic shergottites (abstract #1723). 37th Lunar and Planetary Science Conference. CD-ROM.

Nyquist L. E., Bogard D. D., Shih C.-Y., Greshake A., Stöffler D., and Eugster O. 2001. Ages and geologic histories of Martian meteorites. *Space Science Reviews* 96:105–164.

Ostertag R. 1983. Shock experiments on feldspar crystals. Proceedings, 14th Lunar and Planetary Science Conference. *Journal of Geophysical Research* 88:B364–376.

Ott U. and Löhr H. P. 1992 Noble gases in the new shergottite LEW 88516. *Meteoritics* 27:271.

Ott U., Löhr H. P., and Begemann F. 1988 New noble gas data for SNC meteorites: Zagami, Lafayette, and etched Nakhla (abstract). *Meteoritics* 23:295–296.

Ozima M. and Podosek F. A. 2002. *Noble gas geochemistry.* Cambridge: Cambridge University Press.

Park J., Okazaki R., and Nagao K. 2001. Noble gases in SNC meteorites: Dar al Gani 489, Sayh al Uhaymir 005 and Dhofar 019 (abstract). *Meteoritics & Planetary Science* 36:A157.

Pätsch M., Altmaier M., Herpers U., Kosuch H., Michel R., and Schultz L. 2000. Exposure age of the new SNC meteorite Sayh al Uhaymir 005 (abstract). *Meteoritics & Planetary Science* 35: A124–125.

Patzer A. and Schultz L. 2001. Noble gases in enstatite chondrites I: Exposure ages, pairing, and weathering effects. *Meteoritics & Planetary Science* 36:947–961.

Pellas P., Fieni C., Trieloff M., and Jessberger E. K. 1997. The cooling history of the Acapulco meteorite as recorded by the ^{244}Pu and ^{40}Ar-^{39}Ar chronometers. *Geochimica et Cosmochimica Acta* 61:3477–3501.

Reedy R. C. 1981. Cosmic-ray-produced stable nuclides: Various production rates and their implications. Proceedings, 12th Lunar and Planetary Science Conference. pp. 1809–1823.

Reedy R. C. 1992. Solar-proton production of neon and argon (abstract). 23rd Lunar and Planetary Science Conference. pp. 1133–1134.

Reimold W. U. and Stöffler D. 1978. Experimental shock metamorphism of dunite. Proceedings, 9th Lunar and Planetary Science Conference. pp. 2805–2824.

Rubin A. E., Warren P. H., Greenwood J. P., Verish R. S., Leshin L. A., Hervig R. L., Clayton R. N., and Mayeda T. K. 2000. Los Angeles: The most differentiated basaltic Martian meteorite. *Geology* 28:1011–1014.

Sano Y., Terada K., Takeno S., Taylor L. A., and McSween H. Y. Jr. 2000. Ion microprobe uranium-thorium-lead dating of Shergotty phosphates. *Meteoritics & Planetary Science* 35:341–346.

Scherer P., Schultz L., and Loeken T. 1994. Weathering and atmospheric noble gases in chondrites. In *Noble gas geochemistry and cosmochemistry*, edited by Matsuda J. Tokyo: Terrapub. pp. 43–53.

Schmitt R. T. 1995. Experimentelle und theoretische Untersuchungen zur Stoßwellenmetamorphose von gewöhnlichen Chondriten. Ph.D. thesis, Westfälische Wilhelms-Universität Münster, Germany.

Schmitt R. T. 2000. Shock experiments with the H6 chondrite Kernouvé: Pressure calibration of microscopic shock effects. *Meteoritics & Planetary Science* 35:545–560.

Schnabel C., Ma P., Herzog G. F., Faestermann T., Knie K., and Korschinek G. 2001. ^{10}Be, ^{26}Al, and ^{53}Mn in Martian meteorites (abstract #1353). 32nd Lunar and Planetary Science Conference. CD-ROM.

Schultz L. and Franke L. 2004. Helium, neon, and argon in meteorites. A data collection. *Meteoritics & Planetary Science* 39:1889–1890.

Schultz L. and Stöffler D. 1993. Shock effects and noble gas concentrations in chondrites (abstract). *Meteoritics & Planetary Science* 28:432.

Schultz L. and Weber H. W. 1996. Noble gases in H chondrite meteoroid streams: No confirmation. *Journal of Geophysical Research* 101:21,177–21,181.

Schwenzer S. P. 2004. Marsmeteorite: Edelgase in Mineralseparaten, Gesamtgesteinen und terrestrischen Karbonaten. Ph.D. thesis, Johannes Gutenberg-Universität Mainz, Germany.

Schwenzer S. P., Fritz J., Greshake A., Herrmann S., Jochum K. P., Ott U., Stöffler D., and Stoll B. 2004. Helium loss and shock pressure in Martian meteorites—A relationship (abstract). *Meteoritics & Planetary Science* 39:A96.

Schwenzer S. P., Herrmann S., and Ott U. 2006. Nitrogen and noble gases in ALHA77005, a small Martian meteorite from Antarctica (abstract). *Meteoritics & Planetary Science* 41:A161.

Schwenzer S. P., Herrmann S., Mohapatra R. K., and Ott U. 2007. Noble gases in mineral separates from three shergottites: Shergotty, Zagami, and EETA79001. *Meteoritics & Planetary Science* 37:387–412.

Schwenzer S. P. and Ott U. 2006. Evaluating Kr- and Xe-data in the nakhlites and ALH 84001—Does EFA hide EFM (abstract #1614)? 37th Lunar and Planetary Science Conference. CD-ROM.

Sharp T. G. and De Carli P. S. 2006. Shock effects in meteorites. In *Meteorites and the early solar system II*, edited by Lauretta D. S. and McSween H. Y. Jr. Tucson: The University of Arizona Press. pp. 653–677.

Shukolyukov Yu. A., Nazarov M. A., and Schultz L. 2000. Dhofar 019: A shergottite with an approximately 20 million-year exposure age (abstract). *Meteoritics & Planetary Science* 35: A147.

Shukolyukov Yu. A., Nazarov M. A., and Schultz L. 2002. A new Martian meteorite: The Dhofar 019 shergottite with an exposure age of 20 million years. *Solar System Research* 36:125–135.

Shuster D. L. and Weiss B. P. 2005. Martian surface paleotemperatures from thermochronology of meteorites. *Science* 309:594–597.

Stewart S. T., Seifter A., Kennedy G. B., Furlanetto M. R., and Obst A. W. 2007. Measurements of emission temperatures from shocked basalts: Hot spots in meteorites (abstract #2413). 38th Lunar and Planetary Science Conference. CD-ROM.

Stöffler D., Ostertag R., Jammes C., Pfannschmidt G., Sen Gupta P. R., Simon S. B., Papike J. J., and Beauchamp R. H. 1986. Shock metamorphism and petrography of the Shergotty achondrite. *Geochimica et Cosmochimica Acta* 50:889–903.

Stöffler D., Bischoff A., Buchwald U., and Rubin A. E. 1988. Shock effects in meteorites. In: *Meteorites and the early solar system*, edited by Kerridge J. F. and Matthews M. S. Tucson: The University of Arizona Press. pp. 165–205.

Stöffler D., Keil K., and Scott E. R. D. 1991. Shock metamorphism

of ordinary chondrites. *Geochimica et Cosmochimica Acta* 55: 3845–3867.

Stopar J. D., Taylor G. J., and Norman M. D. 2007. Major and trace elements in nakhlite MIL 03346 with a focus on aqueous alteration products (abstract #1448). 38th Lunar and Planetary Science Conference. CD-ROM.

Swindle T. D., Li B., and Kring D. A. 1996. Noble gases in Martian meteorite QUE 94201 (abstract). 27th Lunar and Planetary Science Conference. pp. 1297–1298.

Swindle T. D., Treiman A. H., Lindstrom D. J., Burkland M. K., Cohen B. A., Grier J. A., Li B., and Olson E. K. 2000. Noble gases in iddingsite from the Lafayette meteorite: Evidence for liquid water on Mars in the last few hundred million years. *Meteoritics & Planetary Science* 35:107–115.

Taylor G. J. and Heymann D. 1969. Shock, reheating, and the gas retention ages of chondrites. *Earth and Planetary Science Letters* 7:151–161.

Taylor L. A., Nazarov M. A., Shearer C. K., McSween H. Y. Jr., Cahill J., Neal C. R., Ivanova M. A., Barsukova L. D., Lentz R. C., Clayton R. N., and Mayeda T. K. 2002. Martian meteorite Dhofar 019: A new shergottite. *Meteoritics & Planetary Science* 37:1107–1128.

Terada K., Monde, T., and Sano Y. 2003. Ion microprobe U-Th-Pb dating of phosphates in Martian meteorite ALH 84001. *Meteoritics & Planetary Science* 38:1697–1703.

Terada K. and Sano Y. 2004. Ion microprobe U-Th-Pb dating and REE analyses of phosphates in the nakhlites Lafayette and Yamato-000593/000749. *Meteoritics & Planetary Science* 39: 2033–2041.

Treiman A. H. 1995. S≠NC: Multiple source areas for Martian meteorites. *Journal of Geophysical Research* 100:5329–5340.

Treiman A. H. 1998. The history of Allan Hills 84001 revised: Multiple shock events. *Meteoritics* 33:753–764.

Treiman A. H. 2005. The nakhlite meteorites: Augite-rich igneous rocks from Mars. *Chemie der Erde* 65:203–270.

Treiman A. H., McKay G. A., Bogard D. D., Mittlefehldt D. W., Wang M.-S., Keller L., Lipschutz M. E., Lindstrom M. M., and Garrison D. 1994. Comparison of the LEW 88516 and ALHA77005 Martian meteorites: Similar but distinct. *Meteoritics* 29:581–592.

Trieloff M., Reimold W. U., Kunz J., Boer R. H., and Jessberger E. K. 1994. ^{40}Ar-^{39}Ar thermochronology of pseudotachylite at the Ventersdorp Contact Reef, Witwatersrand Basin. *South African Journal of Geology* 97:365–384.

Trieloff M., Deutsch A., and Jessberger E. K. 1998. The age of the Kara impact structure, Russia. *Meteoritics & Planetary Science* 33:361–372.

Trieloff M., Jessberger E. K., Herrwerth I., Hopp J., Fiéni C., Ghélis M., Bourot-Denise M., and Pellas P. 2003. Structure and thermal history of the H-chondrite parent asteroid revealed by thermochronometry *Nature* 422:502–506.

Trieloff M., Falter M., Buikin A. I., Korochantseva E. V., Jessberger E. K., and Altherr R. 2005. Argon isotope fractionation induced by stepwise heating. *Geochimica et Cosmochimica Acta* 69: 1253–1264.

Varela M. E., Kurat G., Binnin-Mosbah M., Clocchiatti R., and Massare D. 2000. Glass bearing inclusions in olivine of the Chassigny achondrite: Heterogeneous trapping at sub-igneous temperatures. *Meteoritics & Planetary Science* 35:39–52.

Verchovsky A. B., Ott U., and Begemann F. 1993. Implanted radiogenic and other noble gases in crustal diamonds from northern Kazakhstan. *Earth and Planetary Science Letters* 120: 87–102.

Walton E. L. and Herd D. K. 2007. Localized shock melting in lherzolitic shergottite Northwest Africa 1950: Comparison with Allan Hills 77005. *Meteoritics & Planetary Science* 42:63–80.

Walton E. L., Kelley S. P., and Spray J. G. 2007. Shock implantation of Martian atmospheric argon in four basaltic shergottites: A laser probe ^{40}Ar/^{39}Ar investigation. *Geochimica et Cosmochimica Acta* 71:497–520.

Walton E.L., Shaw C. S. J., and Spray J. G. 2006. Crystallization rates of shock melts in three Martian basalts: Experimental simulation with implications for meteoroid dimensions. *Geochimica et Cosmochimica Acta* 70:1059–1075.

Warren P. H. 1994. Lunar and Martian meteorite delivery services. *Icarus* 111:338–363.

Welten K. C., Caffee M. W., Leya I., Masarik J., Nishiizumi K., and Wieler R. 2003. Noble gases and cosmogenic radionuclides in the Gold Basin L4 chondrite shower: Thermal history, exposure history, and pre-atmospheric size. *Meteoritics & Planetary Science* 38:157–173.

Wiens R. C. and Pepin R. O. 1988. Laboratory shock emplacement of noble gases, nitrogen, and carbon dioxide into basalt, and implications for trapped gases in shergottite EETA79001. *Geochimica et Cosmochimica Acta* 52:295–307.

Xie Z. and Sharp T. G. 2004. High-pressure phases in shock-induced melt veins of the Umbarger L6 chondrite: Constraints of shock pressure. *Meteoritics & Planetary Science* 39:2043–2054.

Xie Z., Sharp T. G., and DeCarli P. S. 2006a. Estimating shock pressures based on high-pressure minerals in shock-induced melt veins of L chondrites. *Meteoritics & Planetary Science* 41:1883–1898.

Xie Z., Sharp T. G., and De Carli P. S. 2006b. High-pressure phases in a shock-induced melt vein of the Tenham L6 chondrite: Constraints on shock pressure and duration. *Geochimica et Cosmochimica Acta* 70:504–515.

Zipfel J. 2000. Sayh al Uhaymir 005/008 and its relationship to Dar al Gani 476/489 (abstract). *Meteoritics & Planetary Science* 35: A178.

Zipfel J., Scherer P., Spettel B., Dreibus G., and Schultz L. 2000. Petrology and chemistry of the new shergottite Dar al Gani 476. *Meteoritics & Planetary Science* 35:95–106.